MATERIALS AND METHODS

There are four main parts of this research: meteorological data analyzing, actual evapotranspiration; rainfall; and water budget. First, the 32-year period 1971-2002 of meteorological data was used to analyze reference evapotranspiration, pan evaporation, and rainfall. Meteorological data in Thailand are recorded from 1971; consequently 32 years is nearly the maximum period of data collection available. Weather data to concern reference evapotranspiration and pan evaporation is from 33 weather stations as present in Figure 3 while rainfall data is from 230 rain gauge stations as present in Figure 4.

Secondly, actual evapotranspiration was calculated by SEBAL and the FAO Penman-Montieth equation. The time period for actual evapotranspiration calculations from SEBAL and from the FAO Penman-Monteith computations is one year (January – December 2002). In the SEBAL method, 27 MODIS images were used for daily actual evapotranspiration estimation, while weather data from 33 weather stations was used to produce daily actual evapotranspiration using the FAO Penman-Monteith equation. Thereafter, actual evapotranspiration values calculated from the FAO Penman-Monteith method were compared with actual evapotranspiration values calculated from SEBAL to determine the suitable actual evapotranspiration for the calculation of water budgets.

Thirdly, rainfall was obtained from TRMM images and rain gauge stations. The time period for rainfall data from TRMM images and from rain gauge stations is one year (January – December 2002). For TRMM images, monthly rainfall maps provided by NASA were used. Recorded daily rainfall from 230 rain gauge stations was used. Thereafter, monthly rainfalls from TRMM image were compared with monthly rainfall from rain gauge station to determine the suitable monthly rainfall for the calculation of water budgets.

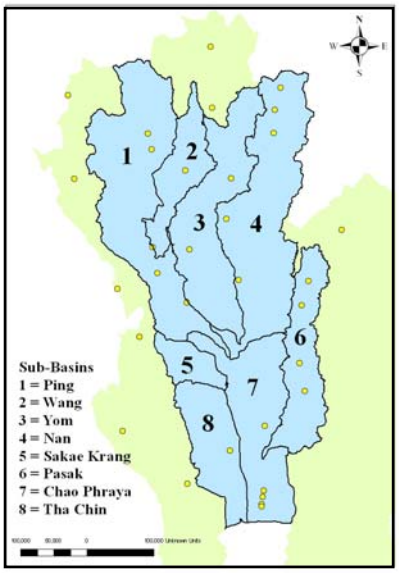

Figure 3 The location of 33 weather stations recorded by the Thai Meteorological Department

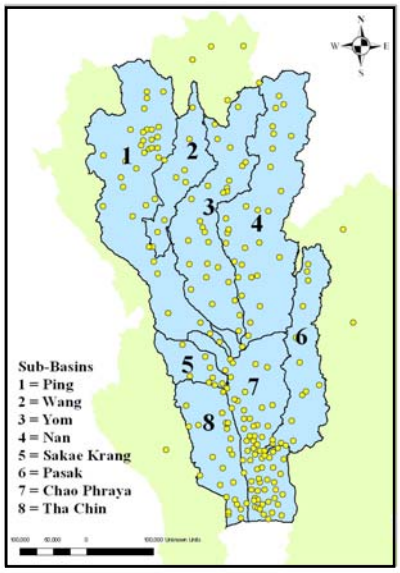

Figure 4 The location of 230 rain gauge stations recorded by the Royal Irrigation Department

Finally, monthly water budgets were calculated in eight sub-basins. These eight sub-basins consist of the Ping, Wang, Yom, Nan, Sakae Krang, Pasak, Tha Chin and Chao Phraya sub-basins. The main inflow for each sub-basin is rainfall, while the main outflow for each sub-basin is actual evapotranspiration. Then, monthly actual evapotranspiration and monthly rainfall in 2002 were utilized for the monthly water budget calculations. Also, spatial and temporal distribution of irrigation requirement was calculated.

Meteorological Data Analyzing

In meteorological data analyzing, daily data of pan evaporation, temperature, relative humidity, wind speed, sun hour, and rainfall during 32-year period (1971 – 2002) was used. The temporal trends of mean annual values of reference evapotranspiration, pan evaporation, and rainfall were not only obtained but the spatial and temporal distributions of mean monthly reference evapotranspiration were also computed. In addition, the relationship of the temporal trends of mean annual value of reference evapotranspiration, pan evaporation, net radiation, temperature, and relative humidity was figured. Reference evapotranspiration was obtained by the FAO Penman-Monteith method. The daily reference evapotranspiration during 1971 to 2002 is result from this calculation. Thereafter, mean monthly reference evapotraspiration was interpolated from point value to be spatial value using the concept of Co-Kriging.

The Calculation of Reference Evapotranspiration (ET_o)

The reference crop evapotranspiration (ET_o) can be calculated on a daily basis using the FAO Penman-Monteith equation (Allen, 2000):

$$ET_o = \frac{0.408\Delta(R_n - G) + \gamma \frac{900}{T_M + 273.2} u_2 (e_s - e_a)}{\Delta + \gamma(1 + 0.34u_2)} \quad (67)$$

where ET_o is reference crop evapotranspiration (mm d^{-1}), R_n is net radiation (MJ $m^{-2}d^{-1}$), G is soil heat flux (MJ $m^{-2}d^{-1}$), T is air temperature (C), e_s is saturation vapor pressure at air temperature (kPa), e_a is vapor pressure of air (kPa), u_2 is wind speed at 2 m (m s^{-1}), Δ is slope of saturation vapor pressure curve at air temperature (kPa C^{-1}), and γ is psychrometer constant (kPa C^{-1}).

For this equation, reference crop evapotranspiration is estimated for a hypothetical short grass with a height of 0.12 m, a surface resistance of 70 s m^{-1}, and albedo of 0.23 (Allen *et al.*, 1998; Allen, 2000). Meteorological factors in order to determine reference crop evapotransiration consist of solar radiation, air temperature, air humidity, and wind speed. All of these factors are applied to the FAO Penman-Monteith equation.

To validate reference evapotranspiration calculated by the FAO Penman-Momteith method, recorded pan evaporation was used. Pan evaporation is the amount of water evaporated during a period (mm/day) with an unlimited supply of water (potential evaporation). It is a function of surface and air temperatures, insolation, and wind, all of which affect water-vapor concentrations immediately above the evaporating surface (Brutsaert, W., 1982; Chen *et al.*, 2005; Chong-yu *et al.*, 2006). On the other hand, reference evapotranspiration is a function of temperature, wind, humidity and net radiation. It can be concluded that there is the relationship between the pan evaporation and reference evapotranspiration. (Humphreys *et al.*, 1994; Grismer *et al.*, 2002; Marco, 2002; Richard *et al.*, 2005) Chong-yu *et al.* (2006) presents that the decreasing trend detected in the pan evaporation and reference evapotranspiration can be attributed to the significant decreasing trends in the net radiation and in the wind speed. Also, it can be attributed to the significant increasing trend in the air temperature.

Daily pan evaporation at 33 weather stations from 1971 to 2002 was used to determine the average of monthly pan evaporation. Thereafter, the correlation

coefficients between mean monthly reference evapotranspiration and mean monthly pan evaporation for 33 weather stations were obtained. The correlation coefficients are from 0.85 to 0.96. The results of correlation coefficient at each weather station are presented in Appendix B.

Co-Kriging Interpolation

The principal weather parameters vary with the characteristic of topography. For example, the decrease of temperature with increasing altitude is known as the environmental lapse rate and is approximately 6.5°C/1000 m (3.5°F/1000 Foot) so reference evapotranspiration is effected by the decrease of temperature (David, 2002). Interpolation schemes are known to have problems from topography, under-sampling, and poorly distributed weather stations. Improved interpolation schemes (e.g., co-kriging with topography) may help to overcome these problems.

Co-kriging is a geostatiatical technique developed to improve the estimation of a variable using the information on other spatially correlated variables which are generally better sampled. Since in-depth discussion about interpolation technique are given by Journel and Huijbregts (1978), Isaaks and Srivastasva (1989), and Burrough and McDonnell (1998), only a briefly describe of the interpolation methods used is presented.

Consider a set of experimental values of monthly reference evapotranspiration or $ET_{o,m}$: [$ET_{o,m,i}$, i = 1, 2, …, 12] and a set of experimental values of elevation or Y: [Y_k, k = 1, 2, …,6252]. 12 is number of month in one year and 6252 is number of elevation point that is converted from an elevation contour map by a grid of 5 km x 5 km. This elevation contour map was supported by Royal Irrigation Department. In this study, the value of $ET_{o,m}$ at space location x_o from $ET_{o,m}$ and Y was estimated. A following equation presents the estimation of $ET_{o,m}$ ($ET^*_{o,m}$) at any point x_o.

$$ET^{*}_{o,m}(x_o) = \sum_{i=1}^{12} \lambda^1_i ET_{o,m}(x_i) + \sum_{k=1}^{6252} \lambda^2_k Y(x_k) \quad (68)$$

where λ^1_i and λ^2_k are the weighing factors for first and second known variables. The biased conditions are thus given as

$$\sum_{i=1}^{12} \lambda^1_i = 1 \quad (69)$$

$$\sum_{k=1}^{6252} \lambda^2_k = 1 \quad (70)$$

The condition of optimality that is minimizing the variance of the estimation error results in the following co-kriging system:

$$\sum_{j=1}^{12} \lambda^1_j \gamma^1_{ij} + \sum_{k=1}^{6252} \lambda^2_k \gamma^{12}_{ik} + \mu_1 = \gamma^1_{io} \quad \text{i= 1,…, 12} \quad (71)$$

$$\sum_{i=1}^{12} \lambda^1_i \gamma^{12}_{ik} + \sum_{i=1}^{12} \lambda^2_i \gamma^2_{ik} + \mu_2 = \gamma^{12}_{ko} \quad \text{k= 1,…, 6252} \quad (72)$$

where γ^1 is the variogram for the first (principal) variable, γ^2 is the variogram for the secondary variable, γ^{12} is the cross-variogram between the first and second variables, and μ_1 and μ_2 are Lagrange multipliers. The variograms is presented by equation 73 and 74 while cross-variograms is defined by equation 75.

$$\gamma^1(h) = \frac{1}{2n}\left[\left(ET_{o,m}(x_i) - ET_{o,m}(x_j)\right)^2\right] \quad (73)$$

$$\gamma^2(h) = \frac{1}{2n}\left[\left(Y(x_i) - Y(x_j)\right)^2\right] \quad (74)$$

$$\gamma^{12}(h) = \gamma^{21}(h) = \frac{1}{2n}\sum_{i=1}^{12}\left[ET_{o,m}(x_i) - ET_{o,m}(x_j)\right]\cdot\left[Y(x_i) - Y(x_j)\right] \quad (75)$$

where h is distance and $ET_{o,m}(x_i), ET_{o,m}(x_j), Y(x_i),$ and $Y(x_j)$ are values of experimental variables $ET_{o,m}$ and Y at space locations $x_i, x_j(x_j + h)$, respectively. The variance of estimation error is given by

$$\sigma^2 = \sum_{i=1}^{12}\lambda_i^1\gamma_{io}^1 + \sum_{k=1}^{6252}\lambda_k^2\gamma_{ko}^{12} + \mu_{01} \quad (76)$$

Actual Evapotranspiration

The estimation of the evapotranspiration for a specific crop requires first calculating potential or reference evapotranspiration and then applying the proper crop coefficients to determine actual evapotranspiration. Potential evapotranspiration is defined as the amount of water transpired in a given time by a short green crop, completely shading the ground, of uniform height and with adequate water status in the soil profile. On the other hand, reference evapotranspiration is defined as the rate of evapotranspiration from a hypothetical reference crop with an assumed crop height of 0.12 m (4.72 in), a fixed surface resistance of 70 sec m^{-1} (21.9 sec ft^{-1}) and an albedo of 0.23, closely resembling the evapotranspiration from an extensive surface of green grass of uniform height, actively growing, well-watered, and completely shading the ground. (Penman, 1948; Allen et. al., 1998) Actual evapotranspiration is defined as the quantity of water that is actually removed from a surface due to the processes of evaporation and transpiration.

Actual Evapotranspiration Calculated by SEBAL

The SEBAL algorithm is a tool to compute actual evapotranspiration for flat areas with the most accuracy and confidence. Satellite image and weather data are

used in the SEBAL model to calculate actual evapotranspiration by using a surface energy balance. SEBAL evaluates an instantaneous actual evapotranspiration flux for the image time, because the satellite image provides information for the overpass time only. The actual evapotranspiration flux can be calculated for each pixel of the image as a residual of the surface energy budget equation (Bastiaanssen, 1998):

$$LE = (R_n - G) - H \tag{77}$$

where LE is the latent energy of evaporation (W/m^2), R_n is the net radiation flux at the soil surface (W/m^2), G is the soil heat flux (W/m^2), and H is the sensible heat flux to the air (W/m^2).

After LE was computed, the Evaporative Fraction (Λ) is the next value that is obtained using Equation 78. The Evaporative Fraction at each pixel of a satellite image can be estimated using the 24-hour evapotranspiration for the day of the image. The Evaporative Fraction is assumed to be a constant value over the full 24-hour period.

$$\Lambda = \frac{LE}{R_n - G} = \frac{LE}{LE + H} \tag{78}$$

To estimate 24-hour actual evapotranspiration, the following equation is utilized.

$$ET_{24} = \frac{86400\Lambda\left(R_{n24} - G_{24}\right)}{\lambda} \tag{79}$$

where R_{n24} is daily net radiation, G_{24} is daily soil heat flux, 86,400 is the number of seconds in a 24-hour period, and λ is the latent heat of vaporization (J/kg). The 24-hour actual evapotranspiration, ET_{24}, can be expressed in mm/day.

Since energy, on average, is stored in the soil during the daytime and released into the air at night, G_{24} is very small for the combined vegetative and soil surface, so it can be assumed as zero at the soil surface (Morse *et al.*, 2000; Hafeez and Chemin, 2002). Then, Equation 79 can be rewritten as:

$$ET_{24} = \frac{86400 \Lambda R_{n24}}{\lambda} \tag{80}$$

Basically, SEBAL is suitable for flat areas but the Chao Phraya River Basin, on which this study is based, includes both flat and mountainous terrain. The Digital Elevation Model or DEM was used to adjust the value in mountain area. DEM is a representation of the topography for the Earth's surface by an array of numbers representing heights above a reference datum. In this research, both contour map elevation and recorded elevation data were used as input data for the GIS software to calculate the spatial DEM in the Chao Phraya River Basin.

For this study, actual evapotranspiration calculated from remote sensing observations was obtained by using SEBAL, MODIS images and Landsat 7 images. Figure 5 presents the concept of actual evapotranspiration calculation using SEBAL, MODIS images and Landsat 7 images. Actual evapotranspiration from Landsat 7 images was used for calibration of that from MODIS images because of the high resolution of Landsat 7 images (30 m. and 60 m.). The above equations are the main equations for actual evapotranspiration calculations from both MODIS and Landsat 7 images. However, there are different equations for detailed calculation as presented in Appendix A.

To calculate actual evapotranspiration using SEBAL, MODIS and Landsat 7 images as input data, ERDAS IMAGINE 8.5 software was used. This software was supported by IWMI. ERDAS IMAGINE 8.5 is a broad collection of software tools designed specifically to process imagery. Imagery is far more than pictures of the earth's surface. It is a valuable source of data that captures actual events at specific times and places in the world. ERDAS IMAGINE 8.5 is software to manipulate and

understand this data. In ERDAS IMAGINE 8.5 software, Spatial Modeler Language was used to write script for actual evapotranspiration computation. The Spatial Modeler Language is a modeling language that is used internally by Model Maker to execute the operations specified in the graphical models.

SEBAL Calculation using MODIS Images

MODIS images were used to estimate 24-hour actual evapotranspiration using the concept of SEBAL. MODIS images were selected for this computation because of their large resolution (250 m, 500 m, and 1 km), which relates to the large area of the Chao Phraya River Basin. A total of 27 MODIS images were used for the actual evapotranspiration computation as shown in Table 12. These 27 MODIS images were selected because they are based on less cloud condition. Also they are distributed in each month.

SEBAL Calculation using Landsat 7 Images

Landsat 7 images were also used to estimate 24-hour actual evapotranspiration by using the concept of SEBAL. Six Landsat 7 images were used for actual evapotranspiration calculation as shown in Table 13. These six Landsat 7 images were selected because they are also based on less cloud condition.

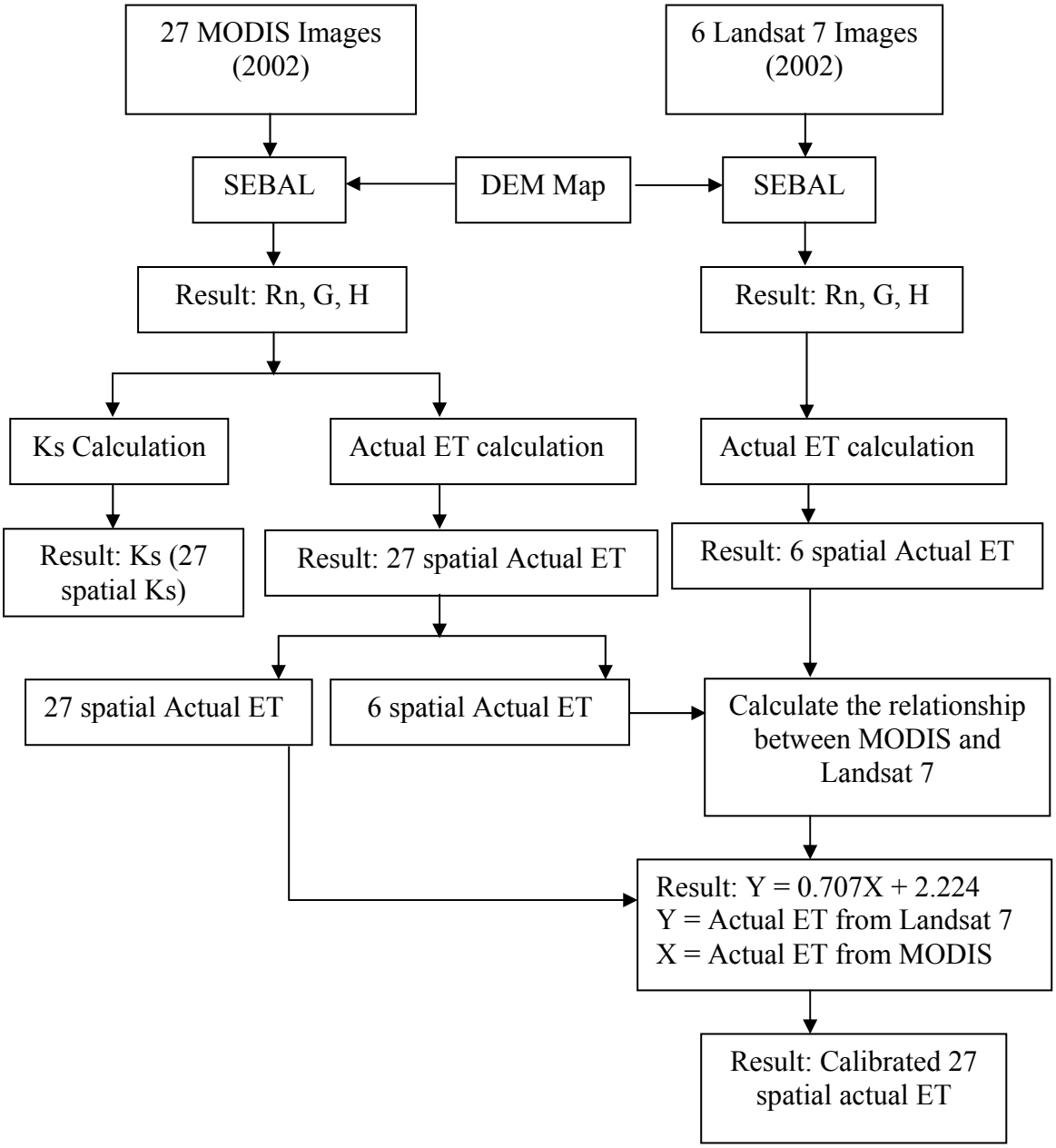

Figure 5 The concept of actual evapotranspiration calculation using SEBAL, MODIS images, and Landsat 7 images

Table 12 The 27 MODIS images used for actual evapotranspiration calculation

Image No.	Date	Image No.	Date	Image No.	Date
1	Jan 3, 02	10	Apr 3, 02	19	Sep 28, 02
2	Jan 17, 02	11	Apr 21, 02	20	Oct 9, 02
3	Jan 26, 02	12	Apr 30, 02	21	Oct 25, 02
4	Feb 2, 02	13	May 2, 02	22	Oct 30, 02
5	Feb 9, 02	14	May 7, 02	23	Nov 6, 02
6	Feb 18, 02	15	Jun 3, 02	24	Nov 5, 02
7	Feb 28, 02	16	Jun 17, 02	25	Nov 20, 02
8	Mar 13, 02	17	Aug 27, 02	26	Dec 1, 02
9	Mar 29, 02	18	Sep 14, 02	27	Dec 8, 02

Table 13 The six Landsat 7 images used for actual evapotranspiration calculation

Image No.	Date	Row/Path
1	Apr 21, 02	48/130
2	Feb 9, 02	49/129
3	Mar 29, 02	49/129
4	May 7, 02	48/130
5	Nov 6, 02	47/131
6	Apr 21, 02	47/130

Calibration

To calibrate actual evapotranspiration of 27 MODIS images, the relationship between 24-hour actual evapotranspiration from six MODIS images and from six Landsat 7 images in the same date was obtained. Landsat 7 (30 m. and 60 m.) image was selected for this calibration because it is included a higher resolution than MODIS image (250 m. and 1000 m.). Before the relationship between actual evapotranspiration from MODIS and Landsat 7 image was obtained, it is important to concern the reliable value of six MODIS image and six Landsat 7 images. To do this,

it was assumed that the actual evapotransapiration of each of the six pairs of MODIS and Landsat 7 images should match because they were all computed by SEBAL. Also, the dates and the locations of the six Landsat 7 images are the same as those of the six MODIS images. The correlation coefficient was used to determine the reliability value of actual evapotranspiration from these 12. The correlation coefficients of actual evapotranspiration for rice, maize, sugarcane, cassava and water were calculated. The correlation coefficients for each crop are 0.654, 0.609, 0.571, 0.649 and 0.659, respectively. The relationship between the actual evapotranspiration from the six MODIS images and the six Landsat 7 images for all crops was obtained using the equation $Y = 0.707X+2.224$ ($R^2 = 0.668$) where Y is the actual evapotranspiration from a Landsat 7 image and X is the actual evapotranspiration from the corresponding MODIS image. After the relationship of actual evapotranspiration from both MODIS and Landsat 7 was determined, 27 MODIS images were adjusted.

Actual Evapotranspiration Calculated by the FAO Penman-Monteith Method

The FAO Penman-Monteith method includes the calculation of actual evapotranspiration (ET_c) that can be estimated from the multiplication of crop coefficient (K_c), soil coefficient (K_s) and reference crop evapotranspiration (ET_o) as following equation. Figure 6 presents the process for actual evapotranspiration calculation using the FAO Penman-Monteith method and weather data.

$$ET_c = K_c \times K_s \times ET_o \tag{81}$$

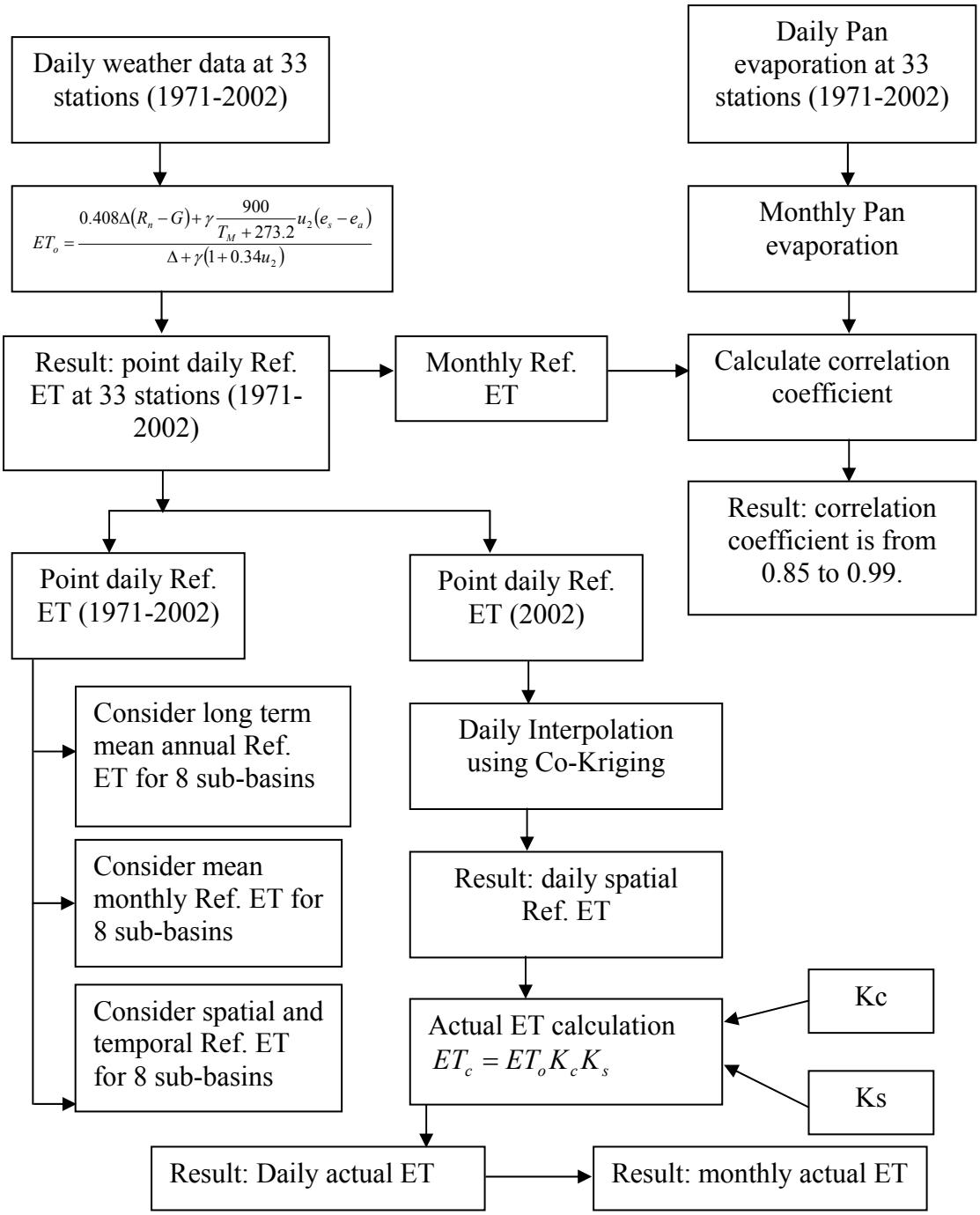

Figure 6 The concept of actual evapotranspiration calculation using the FAO Penman-Monteith method and weather data

The Calculation of Crop Coefficient (K_c)

The crop coefficients (K_c) depend on the crop type and the development of crop. There may be several reference crop values for a single crop depending on the crop's stage of development. For this study, three values of the crop coefficient for description the crop coefficient value were used; those during the initial stage ($K_{c,ini}$), the mid-season stage ($K_{c,mid}$) and the end of the late season stage ($K_{c,late}$) (Allen *et al.*, 1998). Since the crop coefficients represent the crop type, the land use map and the cropping pattern were input data to indicate the crop type for each area. The main crop types cultivated in the study area consist of rice, sugarcane, maize, cassava, fruit tree and small vegetation. Also the crop coefficients depend on the stage of crop development so cropping calendar was used to denote the stage of crop development in one year. The concept of crop coefficient calculation for this research is presented as Figure 7.

The study areas to calculate crop coefficient for rice, maize, and sugarcane consist of the area of the Regional Irrigation Office (RIO) 1, 2, 3, 4 and 10. First, RIO 1 covers Chiang Mai and Lamphun province. Second, RIO 2 covers Phayao, Nan, Chai Rai, and Lampang province. Third, RIO 3 covers Uttardit, Phitsanulok and Nakhon Sawan province. Fourth, RIO 4 covers Phrae, Sukhothai, Tak and Kamphaeng Phet province. Last, RIO 10 covers Phetchabun and Lop Buri province.

Rice, maize, and sugarcane were concerned to calculate crop because these crops are cultivated in the irrigated area and planted nearby a reservoir and nearby a main canal. Also, these crops are in a big area.

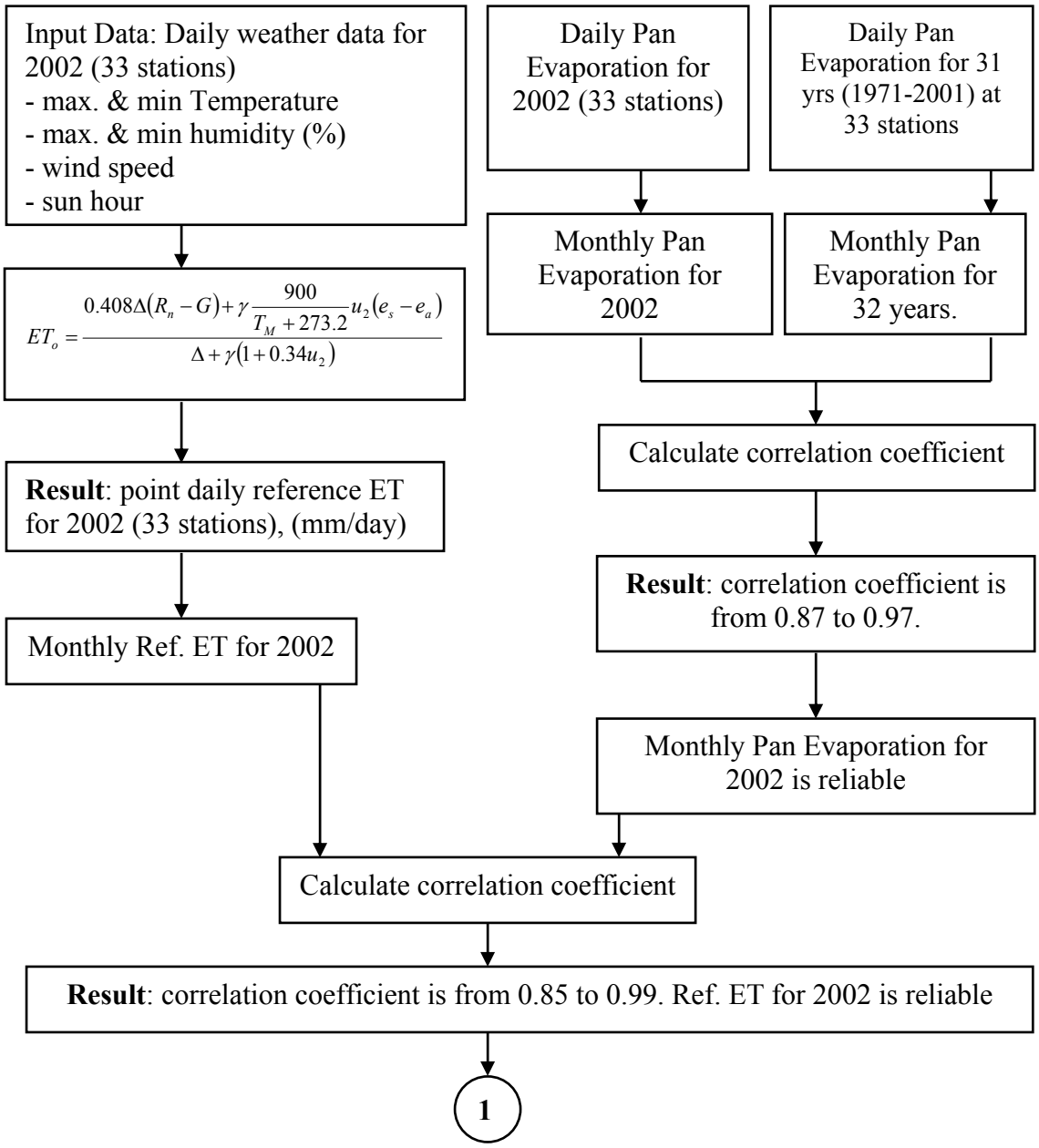

Figure 7 The concept of crop coefficient calculation

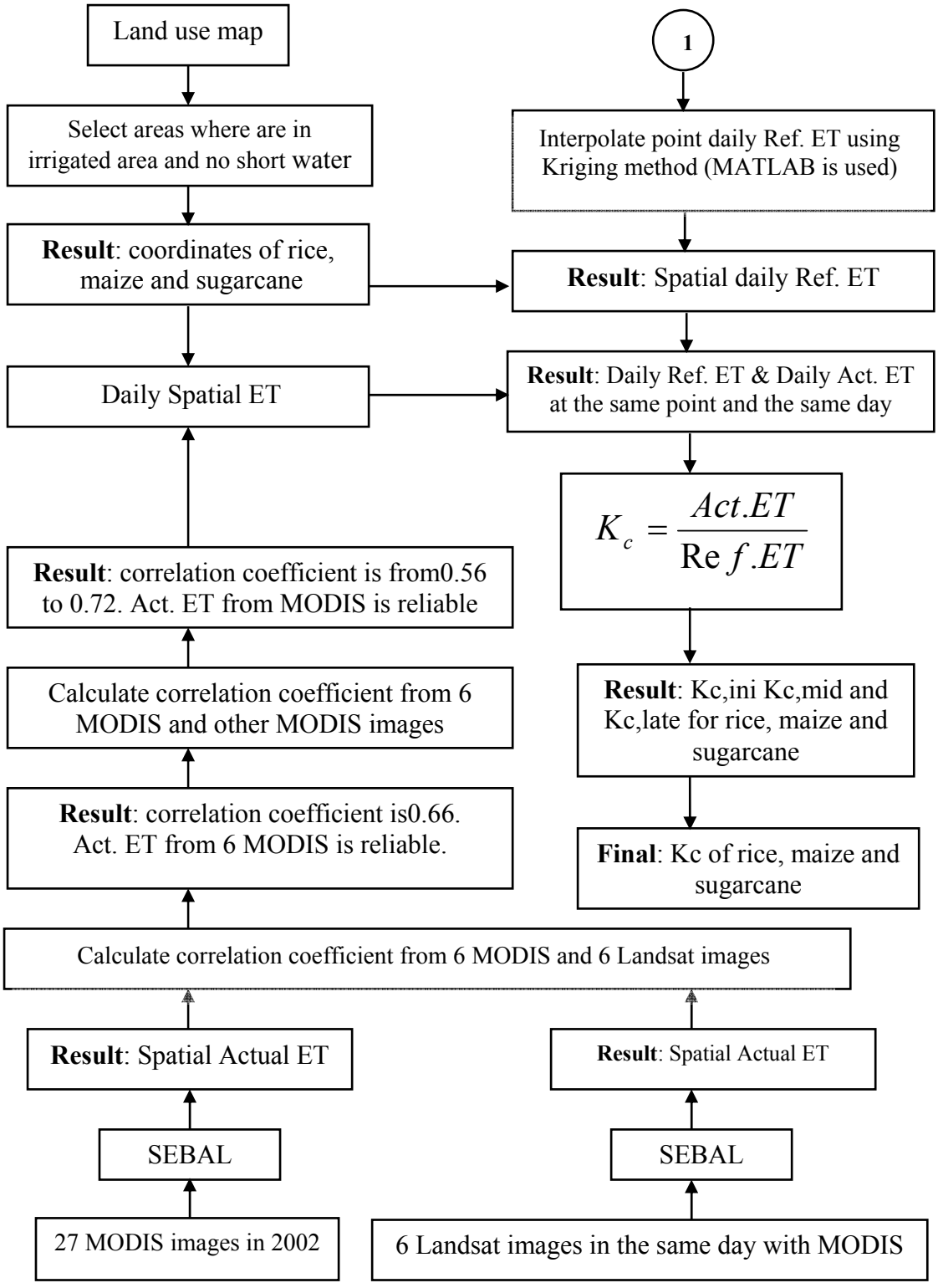

Figure 7 (cont'd)

The locations of rice, maize, and sugarcane were selected by using the map of irrigated area, stream, canal, reservoir, and land use. The locations for rice consist of 63 points while the locations for maize and sugarcane are 52 and 32 points, respectively. The 63 points of rice include five rice cultivars: Suphanburi 1, Chai Nat 1, Ko Kho 10, Ko Kho 7, and Pathumthanee 1. First, Suphanburi 1 is cultivated in Kamphaeng Phet, Nakhon Sawan, and Uttardit province. Second, Chai Nat 1 is planted in Tak, Phitsanulok, Sukhonthai, and Lopburi province. Third, Ko Kho 10 is found in Chai Rai, Chai Mai, Nan, Phrae, Phayao, and Lampang province. Late, Ko Kho 7 and Pathumthanee 1 are cultivated in Lanpun and Phetchabun province, respectively. The lengths of rice development stages are different for each rice cultivars. The lengths from planting to 10% ground cover for Suphanburi 1, Chai Nat 1, Ko Kho 10, Ko Kho 7, and Pathumthanee 1 are 21-28, 56, 35, 7, and 28 days, respectively. The lengths from 10% ground cover to harvest for Suphanburi 1, Chai Nat 1, Ko Kho 10, Ko Kho 7, and Pathumthanee 1 are 120-125, 119-130, 130-135, 120-130, and 120-125 days, respectively. For the locations of maize and sugarcane, there is no data to indicate maize and sugarcane cultivars in each location. Then, crop coefficients for maize and sugarcane are average values for maize and sugarcane cultivars. The average lengths of crop development for each maize and sugarcane cultivars are, respectively, 110-120 and 300-320 days.

The cropping patterns for rice, maize and sugarcane were supported by RIO 1, 2, 3, 4 and 10. Since the cropping pattern of RIO 1 is similar to that of RIO 2, the cropping pattern of RIO 1 and 2 is presented together. In the same reason as RIO 1 and 2, the cropping pattern of RIO 3 and 4 is used together as Table 14.

The crop coefficient can be contained by the following equation (Allen *et al.*, 1998).

$$K_c = \frac{ET_c}{ET_o \times K_s} \tag{82}$$

where ET_c = Actual evapotranspiration (mm), ET_o = Reference evapotranspiration (mm), K_c = Crop coefficient (-) and, and K_s = Soil coefficient (-).

Table 14 The cropping calendar for The Office of Regional Irrigation

RIO	Crop	Wet Season		
		Initial	Mid season	Late
1 & 2	Rice	May	June-September	October
	Maize	April	May-August	September
	Sugarcane	January	February-September	October
3 & 4	Rice	June	July-October	November
	Maize	May	June-September	October
	Sugarcane	April	May-December	January
10	Rice	June	July-October	November
	Maize	May	June-September	October
RIO	Crop	Dry Season		
		Initial	Mid season	Late
1 & 2	Rice	December	January-March	April
	Maize	October	November-February	March
	Sugarcane			
3 & 4	Rice	December	January-March	April
	Maize	November	December-March	April
	Sugarcane			
10	Rice	December	January-April	May
	Maize	November	December-March	April

The actual evapotranspiration is the amount of water that delivered to the air from the process of both evaporation and transpiration. The moisture available, temperature, and humidity are main factors of the actual evapotranspiration. Think of the actual evapotranspiration as water use, that is, water that is actually evaporation and transpiration given the environmental conditions of a place. Since the reference

evapotranspiration is the rate of water lost by well-watered reference crop, to calculate actual evapotranspiration the reference evapotranspiration is adjusted by the crop coefficient and the soil dryness coefficient. The soil coefficient is a function of soil moisture depletion. As soil dries, it is more difficult for plants to withdraw water. This phenomenon is explained by the soil coefficient. For example, if there is 20 percent depletion or the soil profile is 80 percent full, the soil coefficient is less than 1.00. On the other hand, if there is no the soil moisture depletion or the soil profile is 100 percent, the soil coefficient is equal to 1.00 (I. Broner, 2005). For this study, since the study areas are in the irrigated area, nearby the reservoir, or nearby the main canal, it can be assumed that there is no the soil moisture depletion. The soil coefficient equaled to 1.00 was used. Then, the crop coefficient can be estimated as following equation that actual evapotranspiration and reference evapotranspiration are obtained by SEBAL and the FAO Penman-Monteith method, respectively.

$$K_c = \frac{ET_c}{ET_o} \tag{83}$$

As above equation, crop coefficients for rice, maize, and sugarcane were obtained. For rice, calculated crop coefficient of $K_{c,ini}$, $K_{c,mid}$, and $K_{c,late}$ are 0.963, 1.194, and 0.934, respectively, while the $K_{c,ini}$, $K_{c,mid}$, and $K_{c,late}$ for maize are 0.978, 1.185, and 0.897, respectively. For sugarcane, the $K_{c,ini}$, $K_{c,mid}$, and $K_{c,late}$ are 0.811, 1.262, and 1.007, respectively. After crop coefficient for rice, maize, and sugarcane were obtained from this study, these crop coefficient were applied to compute actual evapotranspiration.

In the Chao Phraya River Basin, rice, maize, and sugarcane are not only the main ground cover of this basin but there are also other ground covers such as cassava, forest, fruit, small vegetation, and bare soil. Then, the main ground covers that are rice, maize, sugarcane, cassava, forest, fruit, small vegetation, and bare soil in the Chao Phraya River Basin are concerned crop coefficient. The crop coefficient of cassava and bare soil were obtained from FAO Irrigation and Drainage paper 56

(Allen *et al.*, 1998) while the crop coefficients of forest, fruit, and small vegetation were obtained from Danish Hydraulic Institute (2003). For cassava, crop coefficient are 0.30, 0.80, and 0.30 for $K_{c,ini}$, $K_{c,mid}$, and $K_{c,late}$, respectively, while the crop coefficients for small vegetation are 0.59, 1.12, and 0.72. For forest and bare soil, crop coefficients are constant values that are 1.00 and 0.20, respectively. For fruit, crop coefficients from January to December are 2.3, 2.5, 1.9, 1.7, 1.6, 1.3, 1.2, 1.2, 2.1, 2.5, 2.5, and 2.3, respectively. Figure 8 show the crop coefficient during $K_{c,ini}$, $K_{c,mid}$, and $K_{c,late}$.

The Calculation of Soil Coefficient (K_s)

The soil coefficient (K_s) describes the effect water stress on crop. It's the function of the saturate degree in the root zone (S) or the water depletion in root zone (D). If there is no water stress in cultivated area, the soil coefficients are not necessary to consider. However, cultivated area consists normally of both unsaturated soil and saturate soil so the soil coefficients for each area have to be defined. In Thailand, there is no recorded soil moisture in the root zone so, to solve this problem, R_n, G and H from SEBAL were applied to concern soil coefficient.

Soil moisture in the root zone was calculated as the degree of saturation in the root zone (S) following an empirical equation (Scott et al, 2003).

$$S = \exp\left(\frac{\Lambda - 1}{0.42}\right) \tag{84}$$

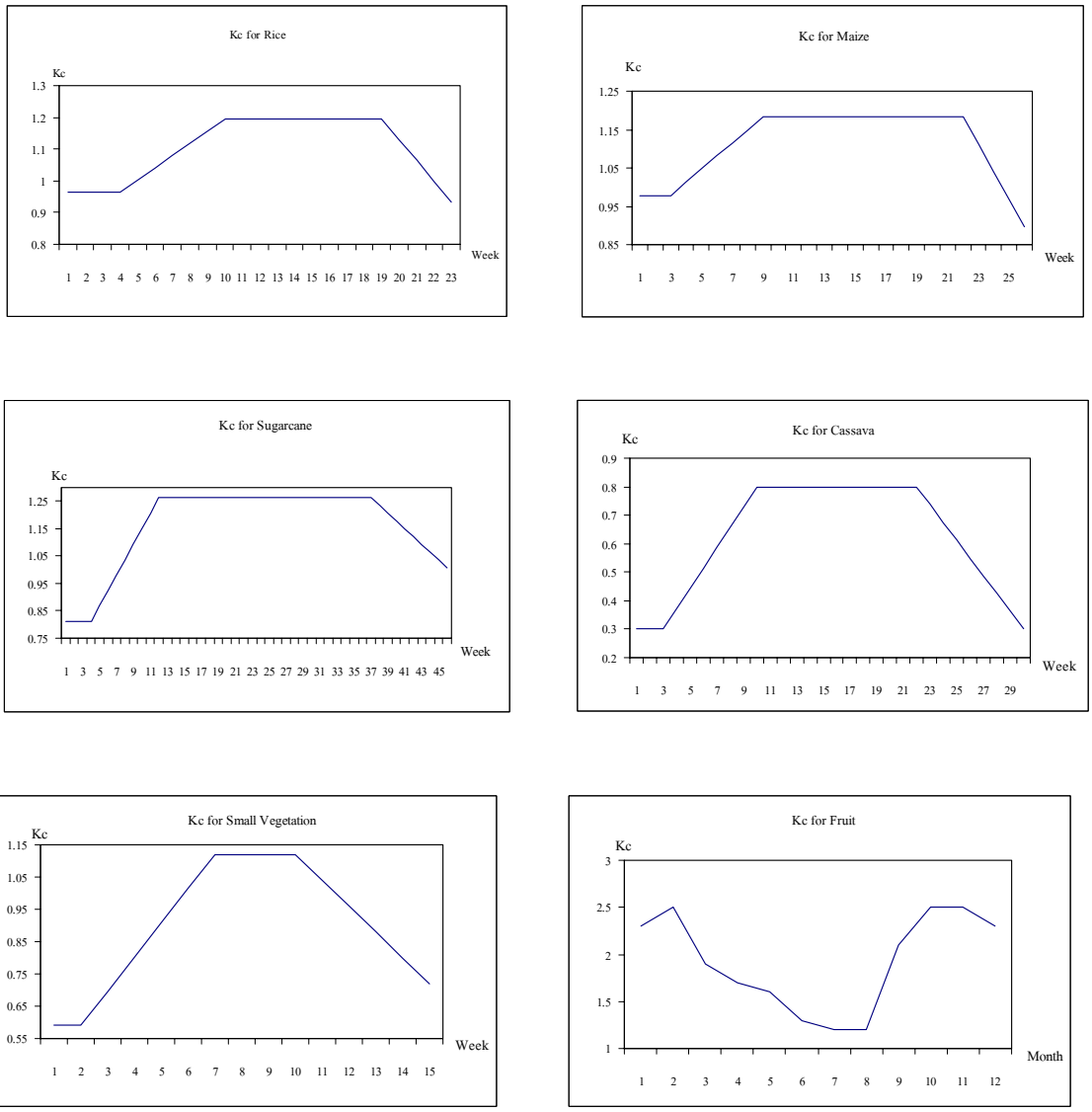

Figure 8 The crop coefficient of rice, maize, sugarcane, cassava, small vegetation, and fruit

From equation 84, the result is from 0.00 to 1.00 that 0.00 is dry soil and 1.00 is saturate soil. However, soil coefficient is the function of the water depletion in root zone (D) so it necessary to cover soil moisture to soil water depletion as Equation 85. Thereafter, soil coefficients were signified by using Table 15 recommended by Broner (2005).

$$D = 1 - S \tag{85}$$

Table 15 The values of soil water depletion (D) and soil coefficient (Ks)

D	K_s	D	K_s	D	K_s
0.00	1.00	0.25	0.94	0.45	0.87
0.05	0.98	0.30	0.92	0.50	0.85
0.10	0.97	0.35	0.92	0.60	0.80
0.15	0.96	0.40	0.89	0.70	0.74
0.20	0.95				

The Comparison between Actual Evapotranspiration Calculated by SEBAL and the Penman-Monteith Method

To determine the linear relationship between the variables of actual evapotranspiration, actual evapotranspiration from SEBAL were compared with actual evapotranspiration from the FAO Penman-Monteith method using the concept of the correlation coefficients. The concept for the comparison is presented in Figure 9. There are 27 days for comparison and there are 30 coordinates used in each day. Appendix Table F2 presents actual evapotranspiration values at 30 coordinates and their correlation coefficients. Also, Figure F1 shows the distribution of these actual evapotranspiration values. The averaged correlation coefficient is 0.79. This result presents that there is a high linear relationship between actual evapotranspiration from SEBAL and the FAO Penman-Monteith method.

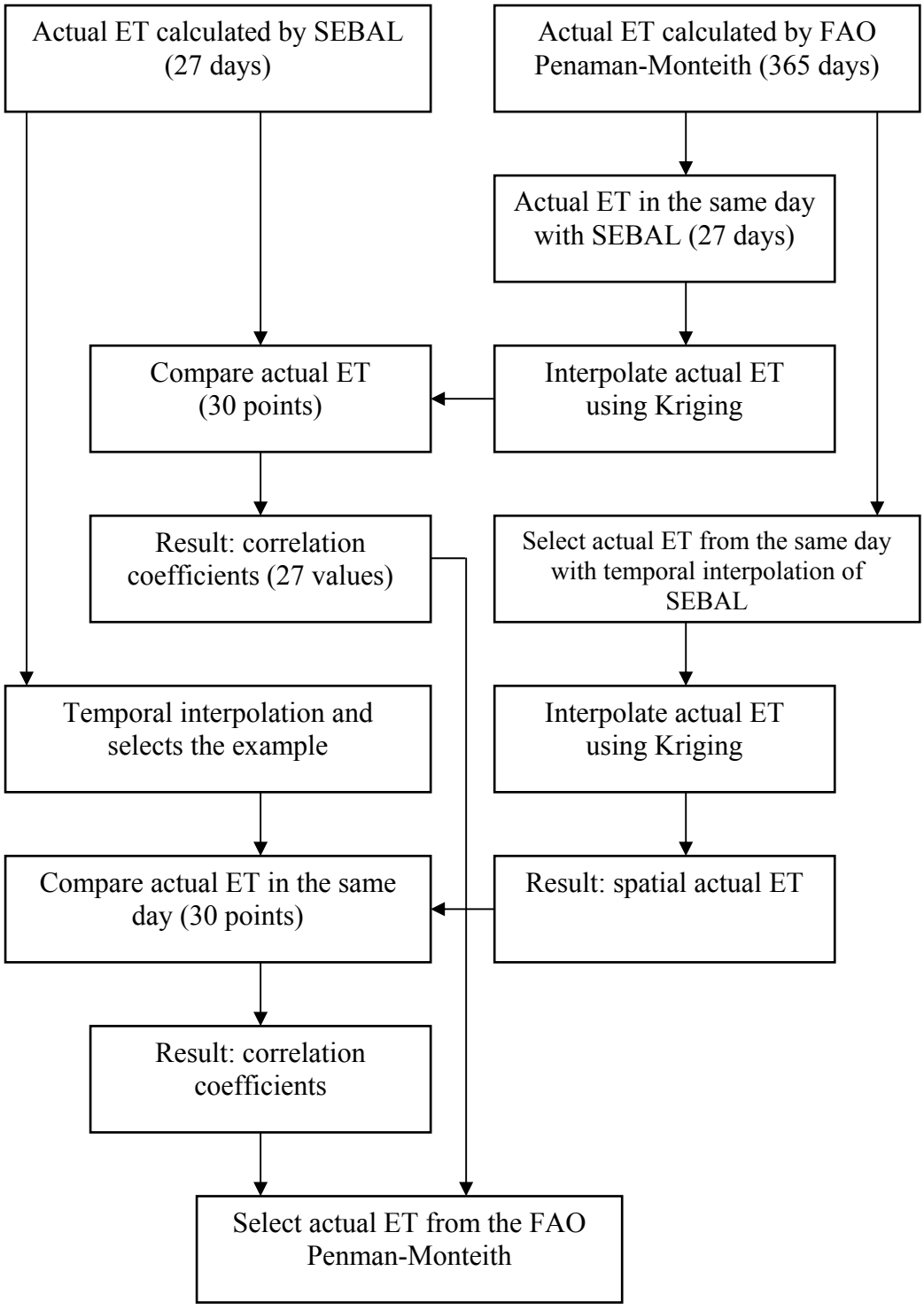

Figure 9 The concept of the comparison between actual evapotranspiration calculated by SEBAL and the FAO Penman-Monteith method

Since actual evpaotranspiration computed by SEBAL was calculated only for 27 days, actual evapotranspiration on other days was determined using the temporal interpolation. Thereafter, the actual evapotranspiration from temporal interpolation were compared with the actual evapotranspiration from the FAO Penman-Monteith method. There are 30 coordinates used for the comparison. Appendix Table F2 presents actual evapotranspiration values and their correlation coefficients and Figure F2 shows the distribution of these actual evapotranspiration values. The averaged correlation coefficient is 0.69. This result presents that there is a high linear relationship between actual evapotranspiration from SEBAL and the FAO Penman-Monteith method.

As above results, it can be seen that the spatial resolution is the advantage of actual evapotranspiration from SEBAL while the temporal resolution is the advantage of actual evapotranspiration from the FAO Penman-Monteith method. Also, actual evapotranspiration from both SEBAL and the FAO Penman-Monteith method can be used in the water budget calculation. For this study, actual evapotranspiration calculated by the FAO Penman-Monteith method was selected to be input data in the water budget calculation because of a good temporal resolution of actual evapotranspiration calculated by the FAO Penman-Monteith method. Actual evapotranspiration from this method during one year was calculated by using recorded weather data. Moreover, there is a high linear relationship between actual evapotranspiration from SEBAL and interpolated actual evapotranspiration from the FAO Penman-Monteith method.

Rainfall

In this part, the rainfall was obtained by rain gauge stations and by TRMM image. Figure 10 presents the process of rainfall analyzing. The recorded daily rainfall data from rain gauge station in one year (January to December 2002) was used. There are 230 rain gauge stations measured by RID. Thereafter, daily rainfall was summarized to be monthly rainfall for each rain gauge station and these monthly rainfalls from all rain gauge stations were interpolated to be spatial monthly rainfall. On the other hand, monthly rainfall from TRMM (3B-42 V6) images, which are provided by NASA at http://disc2.nascom.nasa.gov/Giovanni/tovas/TRMM_V6.3B42_daily.shtml was used. The time period of TRMM images is also one year (January to December 2002). These monthly rainfall images are presented in Figure 11. For the rainfall calculation using TRMM image, Algorithm 3B-42 is used. The Algorithm 3B-42 will use Tropical Rainfall Measuring Mission (TRMM) merged high quality (HQ)/infrared (IR) precipitation and root-mean-square (RMS) precipitation-error estimates to calculate rainfall. These girded estimates are on a 3-hour temporal resolution and a 0.25-degree by 0.25-degree spatial resolution in a global belt extending from 50 degrees south to 50 degrees North latitude. The detail of Algorithm 3B-42 was presented in Appendix C.

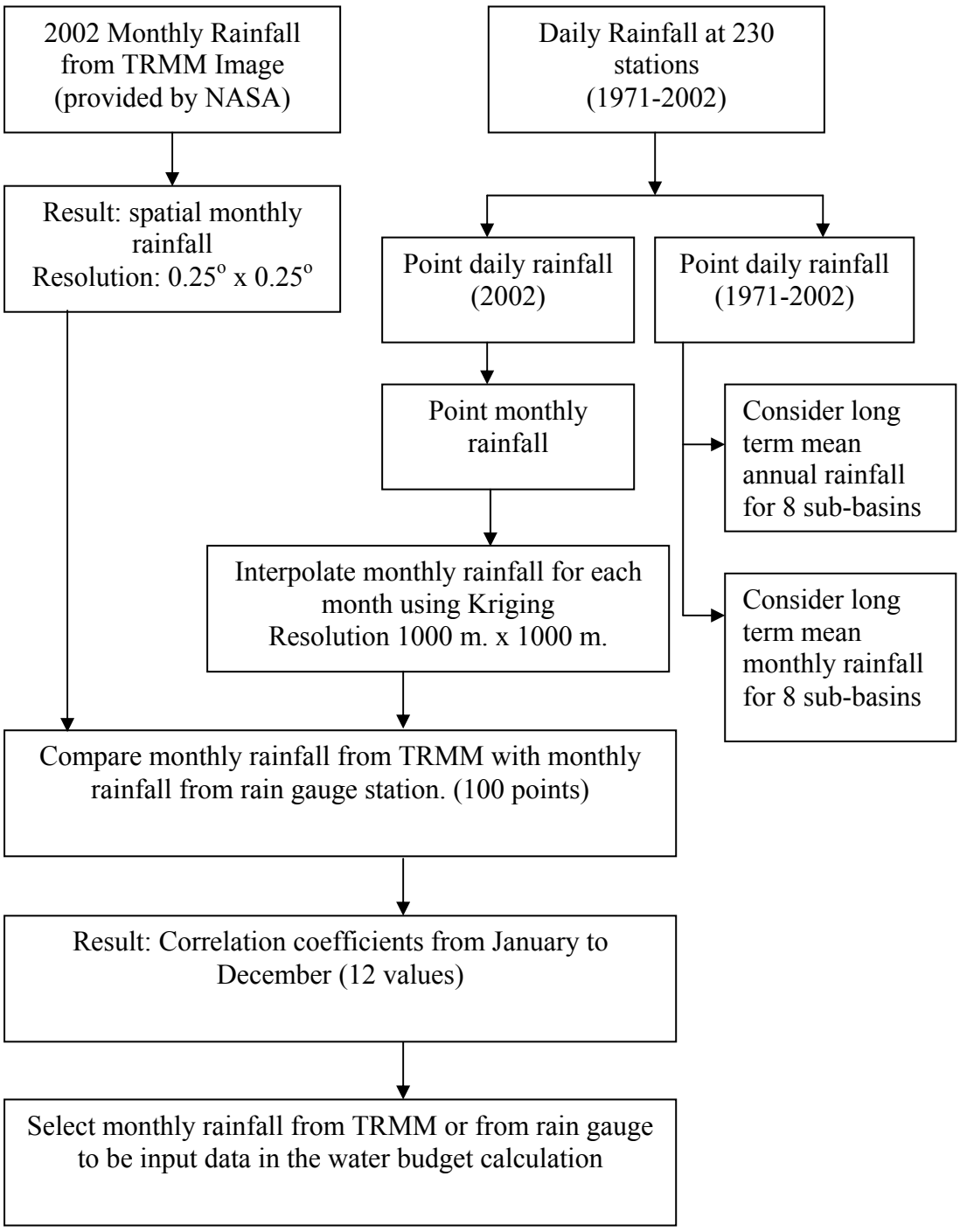

Figure 10 The concept to consider rainfall from rain gauge stations and TRMM (3B42 V6) images

The Calculation of Kriging Interpolation for Rainfall

Monthly rainfall values from 230 rain gauge stations were utilized to interpolate their point rainfall into spatial rainfall using the concept of Kriging interpolation. The resolution of this interpolation is 1000 m. x 1000 m., like the resolution of monthly actual evapotranspiration.

Kriging was used to interpolate point rainfall into spatial rainfall. Kriging is a regression technique used in geostatistics and it is commonly known as Gaussian process regression in the statistical community. Kriging is the estimation method assumed that a weighted average of one or more sample points is the best estimate. Kriging is the method of analysis by which the optimal values of the weights are computed (Clark, 1979 and M. A. Oliver and R. Webster. 1990). The following are main equations for the interpolation of spatial rainfall.

$$R_m(x,y,t_m) = \sum_{i=1}^{n} W_i R(x_i, y_i, t_m) \tag{86}$$

where R_m is estimated rainfall, $R(x_i, y_i, t_m)$ is rainfall and W_i is the kriging weight.

To calculate w_i, sample rainfall have to defined the relationship by semivariogram analysis.

The linear model for a semivariogram has the form

$$\gamma(t) = bt \tag{87}$$

where $\gamma(t)$ is the sample variance of the differences, b is the slope of line, and h is the separation distance from t_i to t_{i+1}.

The nonlinear or power model for a semivariogram has the form

$$\gamma(t) = bt^c \tag{88}$$

where c is the power coefficient.

The exponential model for a semivariogram has the form

$$\gamma(t) = \gamma_r \left[1 - \exp(-\frac{t}{r}) \right] \tag{89}$$

where γ_r is sill, and r is separation distance.

The spherical model for a semivariogram has the form

$$\gamma(t) = \begin{cases} \gamma_r, when(t \succ r) \\ \gamma_r \left(\frac{3t}{2r} - \frac{t^3}{2r^3} \right), when(t \le r) \end{cases} \tag{90}$$

Then

$$\sum_{i=1}^{n} W_i C\left((x_i, y_i, t_t), (x_j, y_j, t_j)\right) + \mu = C\left((x_j, y_j, t_j), (x_o, y_o, t_o)\right) \tag{91}$$

where $C\left((x_i, y_i, t_i), (x_j, y_j, t_j)\right)$ are spatial covariances at different observational locations, $C\left((x_j, y_j, t_j), (x_o, y_o, t_o)\right)$ are covariances between the observation and an estimated field point and μ is Lagrange multiplier in ordinary kriging.

$$\sum_{i=1}^{n} W_i = 1 \tag{92}$$

The Comparison between Monthly Rainfall from TRMM Image and from Rain Gauge Station

To determine the linear relationship between the variables of monthly rainfall, the monthly rainfalls from TRMM image were compared with monthly rainfall from rain gauge station using the concept of the correlation coefficients. For each month, there are 100 coordinates used for comparison and these 100 coordinates are the same location. Appendix Table F3 presents monthly rainfall values at 100 coordinates and their correlation coefficients. Figure F3 shows the distribution of all monthly rainfall values used in the comparison while Figure F4 show the distribution of monthly rainfall used in the comparison from January to December.

The correlation coefficients between monthly rainfall from TRMM images and from rain gauge stations in each month were determined. The result is that the correlation coefficients from January to December consist of 0.87, 0.63, 0.73, 0.78, 0.49, 0.81, 0.48, 0.53, 0.84, 0.73, 0.87, and 0.85, respectively. This result presents that there is a high linear relationship between monthly rainfall from TRMM image and from rain gauge station. Thus, monthly rainfall from both TRMM image and rain gauge station can be used in the calculation water budget.

For this study, monthly rainfall from TRMM image was selected for the water budget calculation because TRMM image covers all study area, especially in the area where there is no rain gauge station such as in the mountain area. Furthermore, spatial resolution is the advantage of monthly rainfall from TRMM.

Water Budget

In hydrological cycle, water is always in movement and the hydrological cycle is described by the continuous movement of water on, above and below the Earth's surface. There is no beginning or end in the hydrological cycle because it is truly a cycle. Water is evaporated from the land and ocean by the latent heat and the water vapor rises. Thereafter, it condenses into clouds and they will be rain. The rain hits

the ground and part runs off, part infiltrates into the ground, and part evaporates back up into the sky. The water from soil will be taken by the plants and vegetation and the water will be released into the air through transpiration. Other parts of the ground water enter streams and flows onto the surface. Eventually, the surface water that runs off in streams, towards the ocean, will be evaporated and continued the cycle. To concern the amount of water in the hydrological cycle, the concept of the water budget is considered. (Molden, 1997; Natalia et. al, 2004)

The water budget concerns the amount of water entering a system (through rainfall and river and groundwater flows) and the amount leaving a system (through evaporation, plant transpiration and river and groundwater flows) as presented in Figure 12.

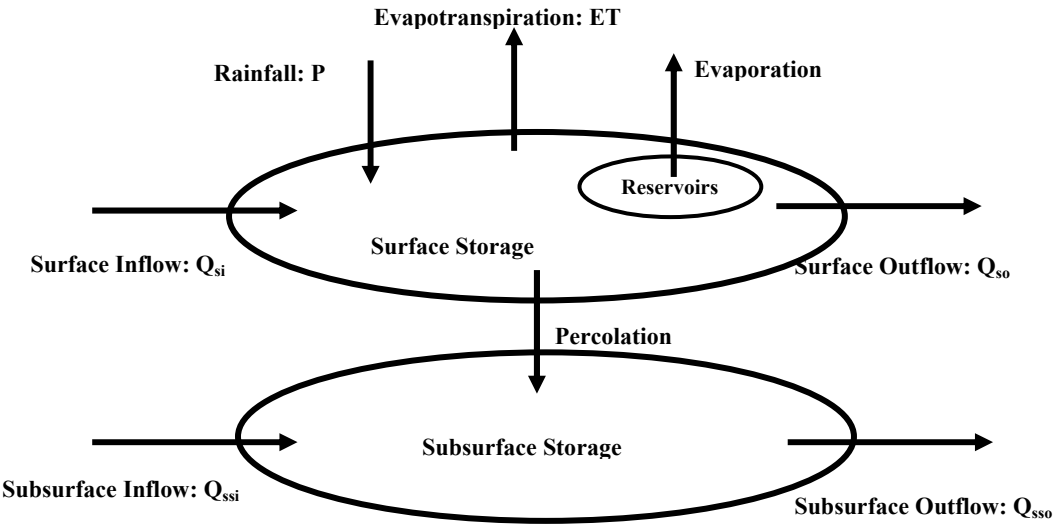

Figure 12 The components of water budget concept

The water budget may be expressed as following equation

$$\left(P + Q_{si} + Q_{ssi}\right) - \left(ET + Q_{so} + Q_{sso}\right) = \Delta S \qquad (93)$$

where P is rainfall (mcm), Q_{si} is surface inflow (mcm), Q_{ssi} is subsurface inflow (mcm), ET is evapotranspiration (mcm), Q_{so} is surface outflow (mcm), Q_{sso} is subsurface outflow (mcm), and ΔS is change in storage within the domain that consists of change in surface water, subsurface water and percolation.

For this study, the domain of interest at each site represents a sub-basin that consists of agricultural, municipal, industrial and forest uses of water. The size of each sub-basin is sufficient to analyze separately from the entire basin in which it is located. The lower boundary extends to the bottom of the aquifer, while the upper boundary is above the crop canopy. The time period of interest is from January to December in 2002.

To compute water budget in eight sub-basins, Ping, Wang, Yom, Nan, Sakae Krang, and Pasak sub-basin were thought as the upper sub-basin because they are included no surface inflow at the apex of their sub-basins. Water budget in Wang sub-basin was firstly computed to determine subsurface outflows and the change in storage for each month. The subsurface and surface outflows of this sub-basin were side flow entering Ping sub-basin. Water budget in Ping sub-basin was then calculated to concern subsurface outflows and the change in storage. Thereafter, the water budgets in Yom, Nan, Sakae Krang, and Pasak sub-basin were also calculated to obtain subsurface outflows and the change in storage for each sub-basin. Finally, subsurface and surface outflows from Ping, Yom, Nan, Sakae Krang, and Pasak sub-basin were inflow entering Chao Phraya sub-basin. For surface inflow entering Tha Chin sub-basin, water was diverted from Chao Phraya sub-basin. Since it's difficult to separate subsurface inflow between Tha Chin and Chao Phraya sub-basin, water budget of these two sub-basins was calculated together. Then, surface outflow and the change in storage of two sub-basins were results.

The concept for water budget calculation for this study is presented as Figure 13. In the upper watersheds, the surface inflow (Q_{si}) and the subsurface inflow (Q_{ssi}) equals to zero. The rainfall was derived from meteorological data and TRMM (3B42

V6) image while the actual evapotranspiration was derived from MODIS satellite imagery, as well as from meteorological data. This actual evapotranspiration was for non-irrigated, irrigated and forest area. However, it can be presented the evaporation from reservoirs and bare soil. The surface outflow (Q_{so}) was obtained from existing stream gauging records that are consisted of P17, W4A, Y17, N10A, CT8, and S2 station for Ping, Wang, Yom, Nan, Sakae Krang, and Pasak sub-basin, respectively. For surface outflow of Chao Phraya and Tha Chin sub-basin, Molle (2001) said that, to control the intrusion of saline water, minimum flows for the Chao Phraya and Tha Chin Rivers are respectively 50 and 35 m^3/s. Also, the main difficulty is that the discharge of the Chao Phraya and Tha Chin Rivers at its mouth cannot be easily measured because of the effect of tidal. Then, minimum flows (50 and 35 m^3/s) are used in this study. The subsurface outflows (Q_{sso}) and the change in storage (ΔS) were derive by the concept of trial and error under the condition assumed that annual change in storage for each sub-basin equal to zero because storage value recovers close to zero at the beginning of each year. Since the subsurface water and the change in storage are results of this computation, it's important to validate the significance level of these results using the statistical significance.

Validation

The subsurface water and the change in storage were validated by the significance level using the statistical significance. In normal English, "significant'' means important, while in Statistics "significant" means probably true (not due to chance). A research finding may be true without being important. When statisticians say a result is "highly significant" they mean it is very probably true. They do not (necessarily) mean it is highly important. Then, significance is a statistical term that tells how sure you are that a difference or relationship exists.

To determine the significant level, the concept of t-test was concerned. The t-test assesses whether the means of two groups are statistically different from each other. This analysis is suitable whenever the means of two groups is compared. The

equation for the t-test is a ratio between the difference of two means or average and a measure of the variability or dispersion of the scores. The t-test equation can be presented by following equation

$$t = \frac{\overline{X}_1 - \overline{X}_2}{\sqrt{\left(\frac{(N_1-1)S_1^2 + (N_2-1)S_2^2}{N_1+N_2-2}\right)\left(\frac{N_1+N_2}{N_1N_2}\right)}} \tag{94}$$

and

$$df = N_1 + N_2 - 2 \tag{95}$$

where df is degrees of freedom, $\overline{X}_1$ and $\overline{X}_2$ are the mean of 1st and 2nd group data, respectively, N_1 and N_2 are the size of 1st and 2nd group data, respectively, and S_1^2 and S_2^2 are the variance of 1st and 2nd group data, respectively, that can be computed by following equation

$$S^2 = \frac{N\sum X^2 - \left(\sum X\right)^2}{N(N-1)} \tag{96}$$

After t and df are calculated by above equations, they are used in Appendix Table D1 to determine the significance level.

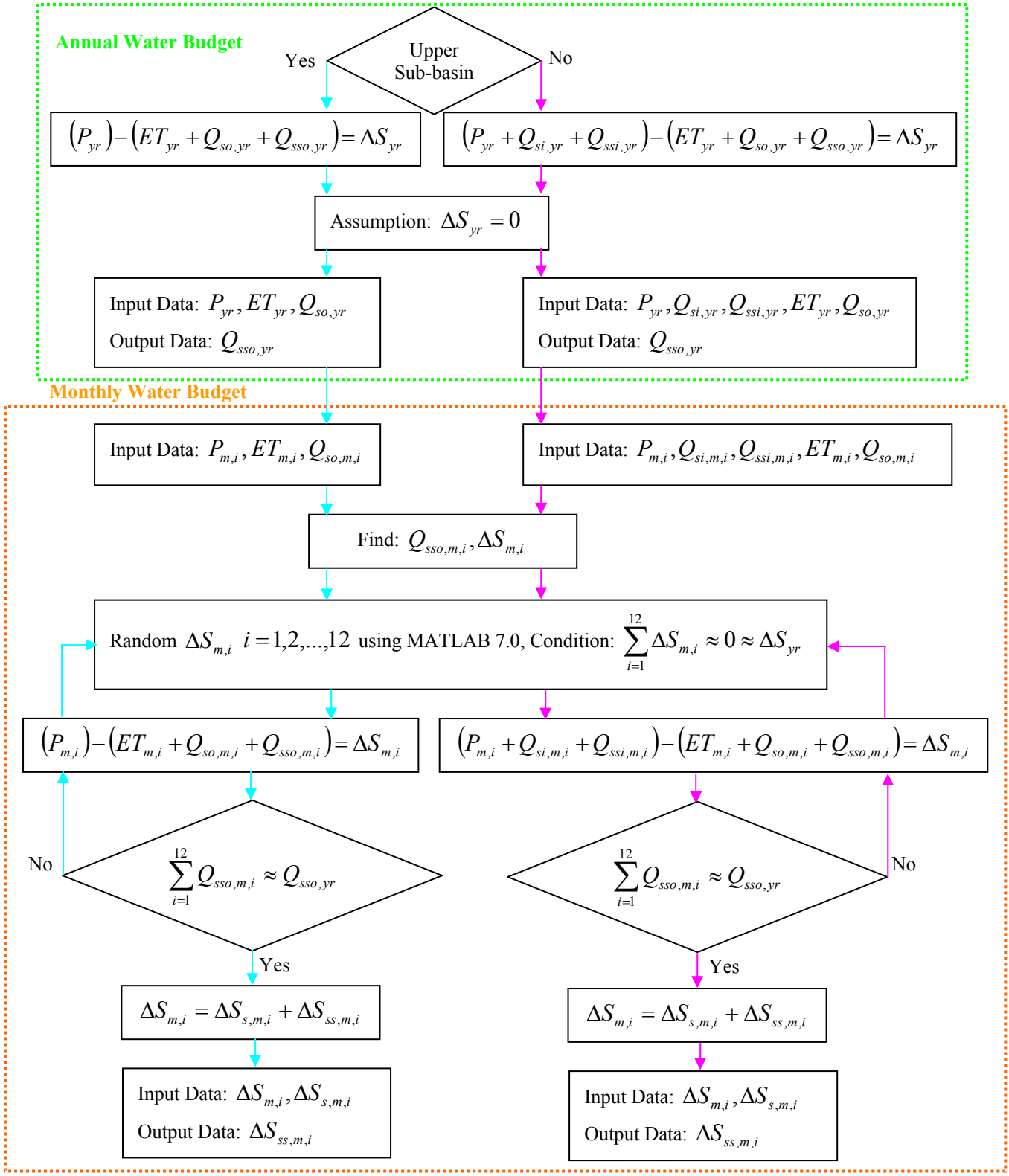

Figure 13 The concept of water budget computation

RESULTS AND DISCUSSION

Since there are four main parts for the calculation of this study, there are four main parts of the result that are the results from evapotranspiration, rainfall, and water budget. The results for each part are presented as following.

Meteorological Data Analyzing

Temporal Trends in Mean Annual Reference Evapotranspiration and Pan Evaporation

The time series of annual reference evapotranspiration and annual pan evaporation from 1971 and 2002 averaged over 8 sub-basins are plotted in Figure 14 and 15. It is seen that both the mean annual reference evapotranspiration and mean annual pan evaporation in all the sub-basins have decreased during a 32-year period. The cause of variability in temporal trends is the meteorological variables in different regions (see Figure 16 - 18). The mean annual net radiation in all sub-basins has decreased during a 32-year period while the mean annual temperature and relative humidity in all sub-basins have increased during a 32-year period. For mean annual reference evapotranspiration, the decreasing trend is the weakest in the Chao Phraya sub-basin and becomes stronger in the Sakae Krang sub-basin. For mean annual pan evaporation, the decreasing trend is also the weakest in the Wang sub-basin and becomes stronger in the Sakae Krang sub-basin. The strongest and weakest of decreasing trend for net radiation are respectively in the Chao Phraya and Nan sub-basin. The strongest and weakest of increasing trend for temperature are in Sakae Krang and Nan sub-basin, respectively, while the strongest and weakest of increasing trend for relative humidity are respectively in Nan and Tha Chin sub-basin.

The maximum values of mean annual reference evapotranspiration, pan evaporation, net radiation, temperature, and relative humidity are in Chao Phraya, Tha Chin, Chao Praya, Tha Chin, and Sakae Krang sub-basin, respectively. However, the minimum values of mean annual reference evapotranspiration, pan evaporation, net radiation, temperature, and relative humidity are, respectively, in Sakae Krang, Sakae

Krang, Wang, Wang, and Nan. The decreasing trend in the mean annual reference evapotranspiration and mean annual pan evaporation differs in different regions. This is logical because it is well-known that the ratio of reference evapotranspiration to pan evaporation, called the pan evaporation coefficient, is not a constant in either region or season (Lui *et al.*, 2004 and Chen *et al.*, 2005).

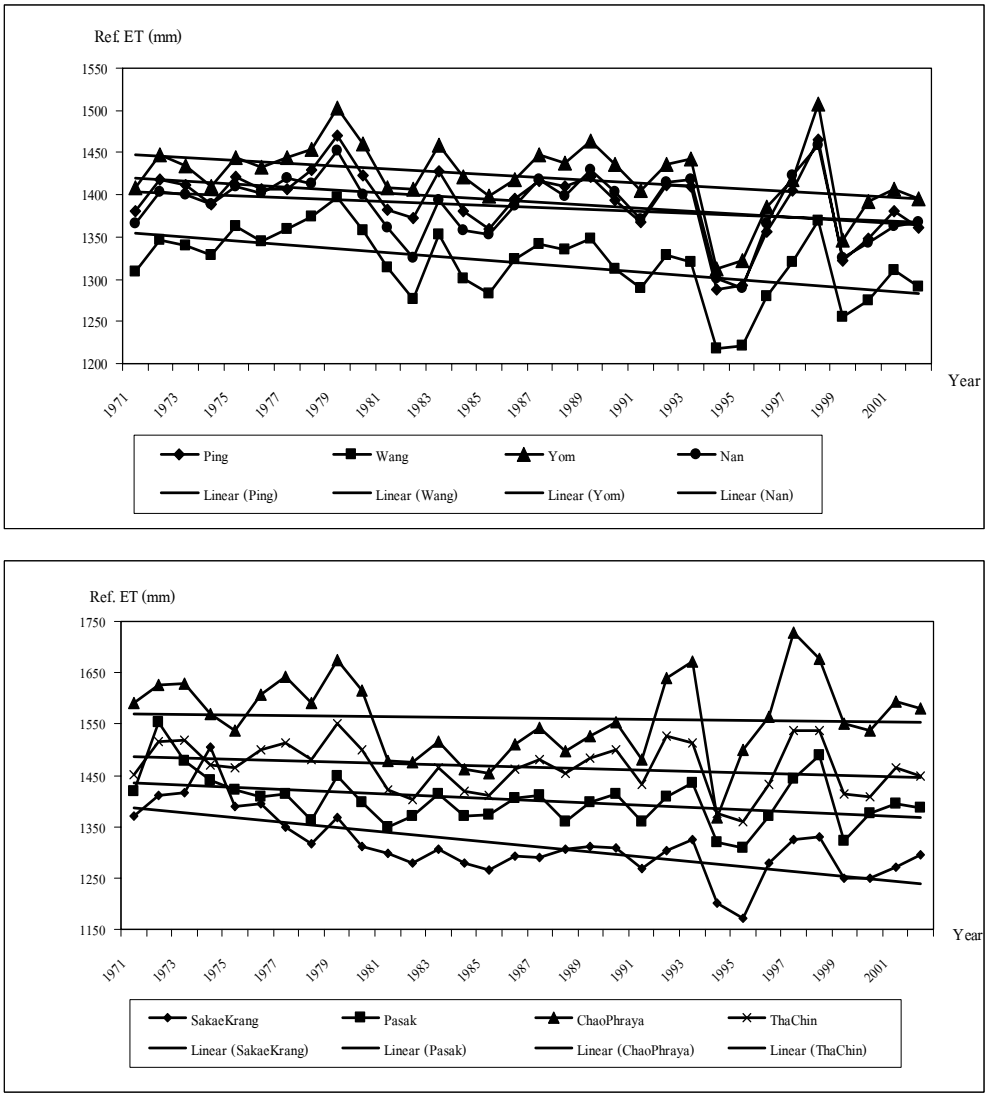

Figure 14 Mean annual reference evapotranspiration and their linear trends in the Ping, Wang, Yom, Nan, Sakae Krang, Pasak, Chao Phraya, and Tha Chin sub-basin

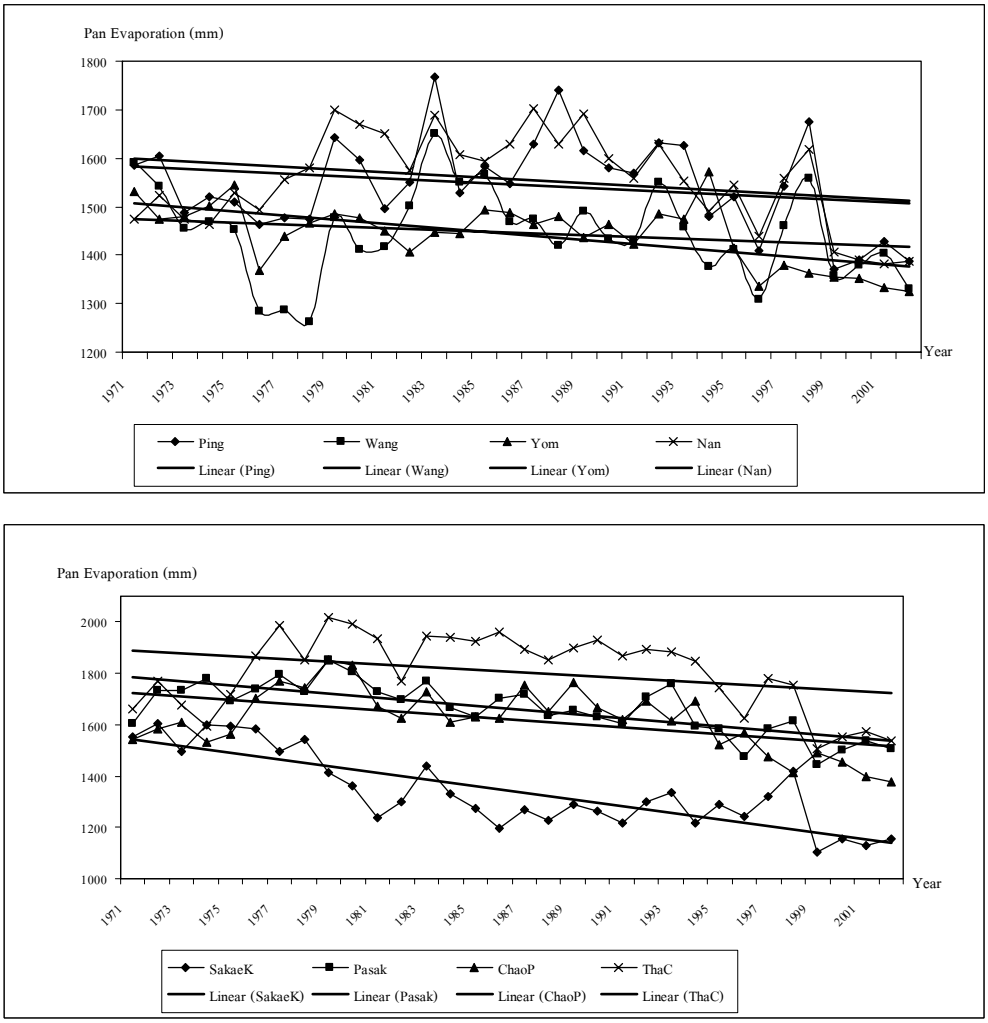

Figure 15 Mean annual pan evaporation and their linear trends in the Ping, Wang, Yom, Nan, Sakae Krang, Pasak, Chao Phraya, and Tha Chin sub-basin

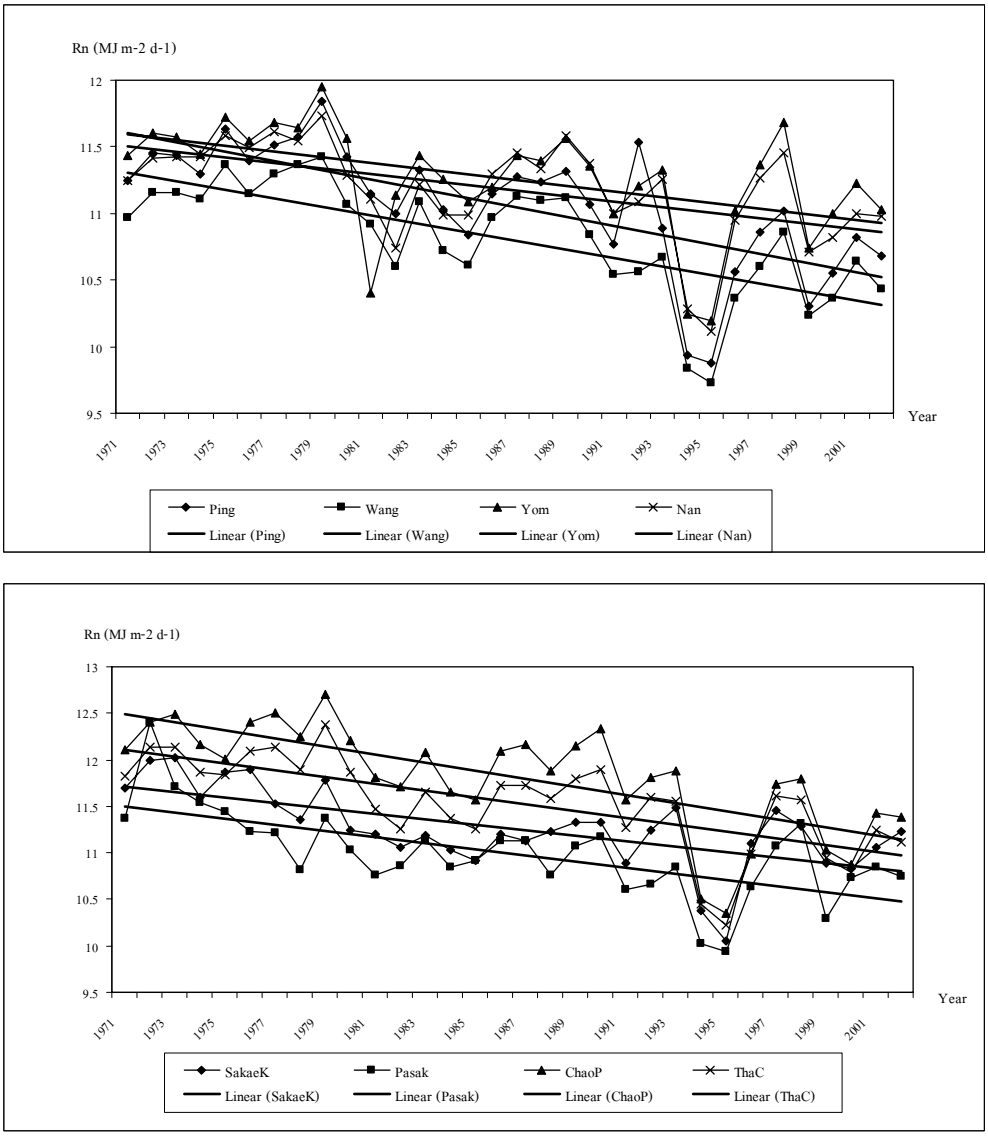

Figure 16 Mean annual net radiation (Rn) and their linear trends in the Ping, Wang, Yom, Nan, Sakae Krang, Pasak, Chao Phraya, and Tha Chin sub-basin

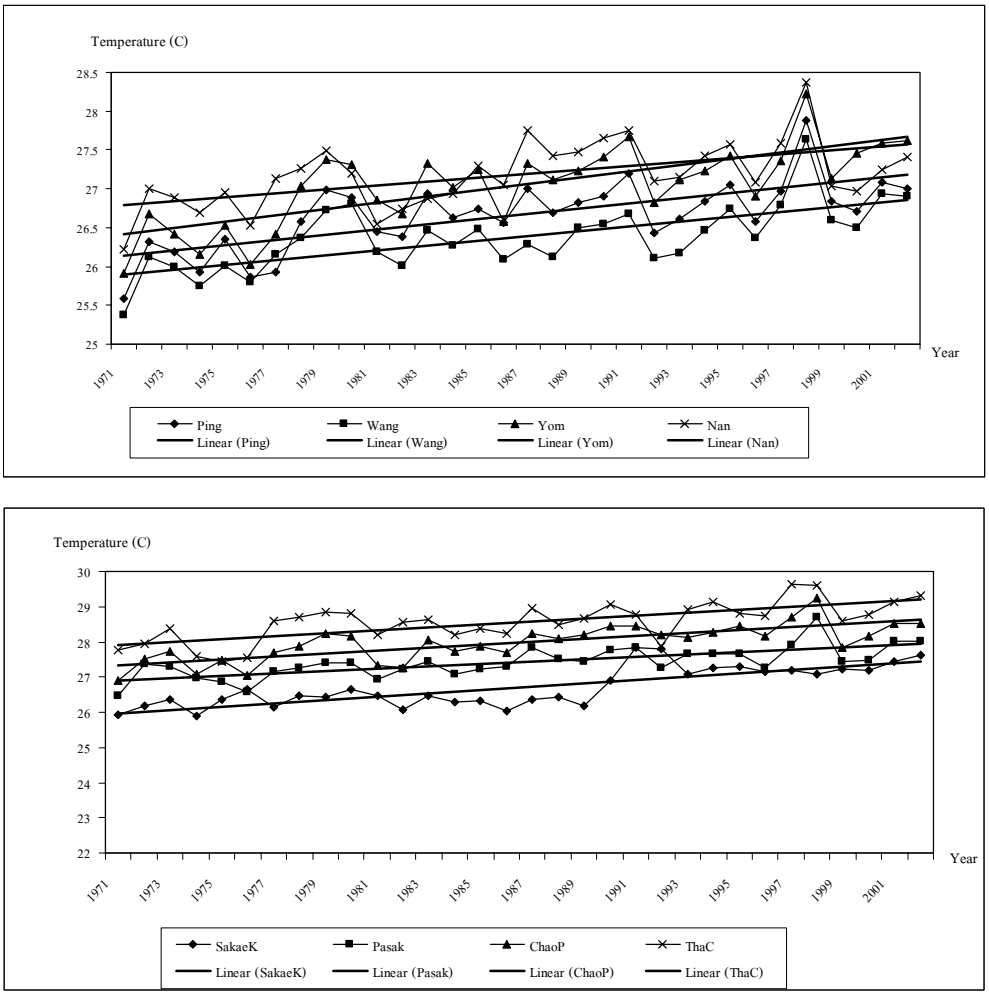

Figure 17 Mean annual temperature and their linear trends in the Ping, Wang, Yom, Nan, Sakae Krang, Pasak, Chao Phraya, and Tha Chin sub-basin

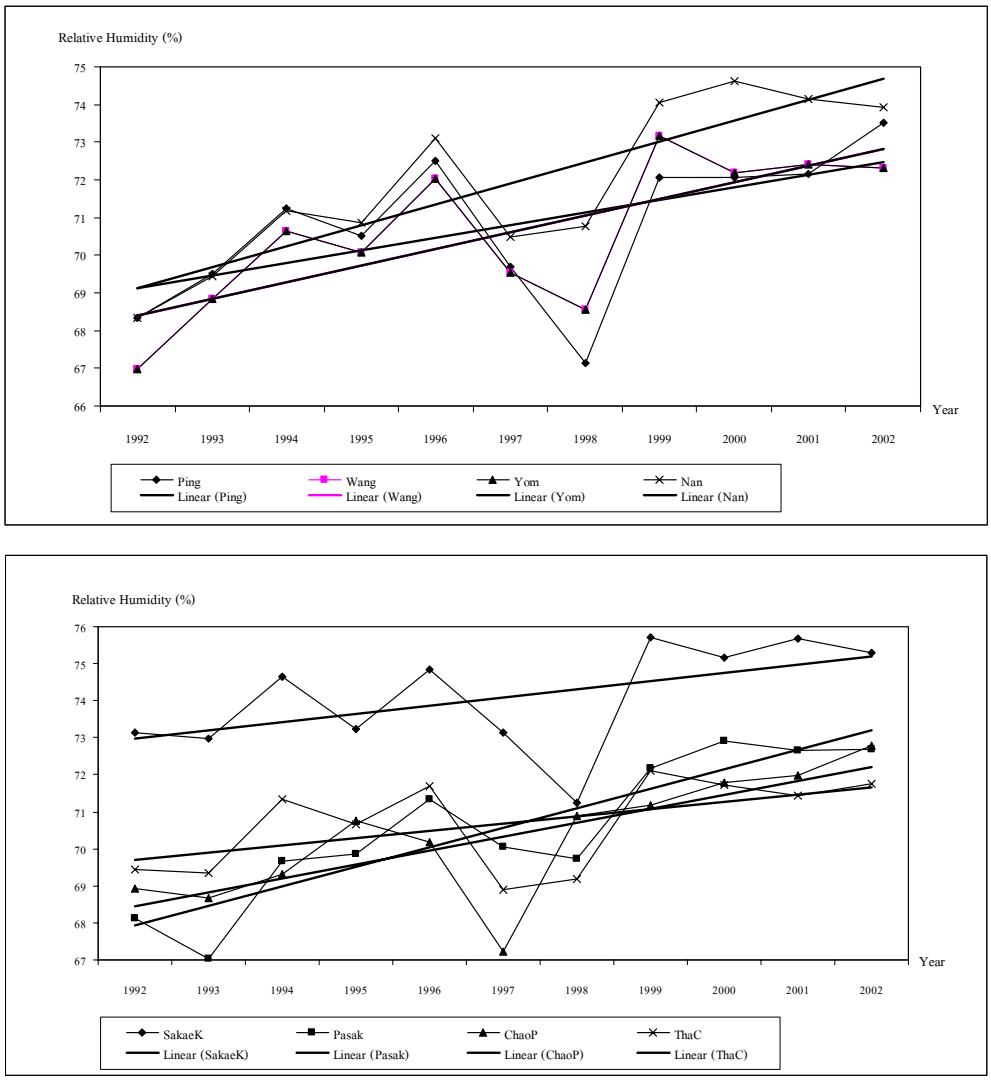

Figure 18 Mean annual relative humidity and their linear trends in the Ping, Wang, Yom, Nan, Sakae Krang, Pasak, Chao Phraya, and Tha Chin sub-basin

Spatial and Temporal Distribution of Mean Monthly Reference Evapotranspiration

The spatial distributions of mean monthly reference evapotranspiration calculated by a 32-year period of weather data are presented in Figure 19. This figure shows the changing of spatial reference evapotranspiration distribution from January to December.

In January, the highest values are found in some area of the Ping and Sakae Krang sub-basin. In February, the highest values are found in the Ping, Tha Chin, Chao Phraya and Sakae Krang sub-basin. In March, reference evapotranspiration in many areas is more than 110 mm. During April to August, the highest value can be found in many areas of Yom, Sakae Krang, Tha Chin, and Chao Phraya sub-basin. Addition, the pattern of reference evapotranspiration distribution during April to August is similar although there is a different value of the highest reference evapotranspiration during these four months. In September, reference evapotranspiration, which is more than 60 mm, distribute in many areas. In October, the highest value can be found in the Ping sub-basin. Moreover, reference evapotranspiration, which is more than 70 mm, distribute in Ping, Yom, Sakae Krang, Pasak, Tha Chin, and Chao Phraya sub-basin. In November, the highest value can be found in the Ping, Wang, and Yom sub-basin. The reference evapotranspiraton though the study area is more than 60 mm. In December, the highest value can be found in the Ping sub-basin. Moreover, reference evapotranspiration, which is more than 60 mm, distribute in Ping, Yom, Sakae Krang, Pasak, Tha Chin, and Chao Phraya sub-basin.

The temporal distribution of mean monthly reference evapotranspiration is plotted as Figure 20. The cause of variability in temporal distributions is also the meteorological variables in different regions (see Figure 21-24).

The mean monthly reference evapotranspiration in the lower Chao Phraya River Basin is higher than that in the upper Chao Phraya River Basin while the mean monthly reference evapotranspiration in the whole catchment is between the upper Chao Phraya River Basin and the lower Chao Phraya River Basin. In Figure 21-24, temperature and net radiation in the lower Chao Phraya River Basin are also higher than that in the upper Chao Phraya River Basin while the values in the whole catchment are also between the upper Chao Phraya River Basin and the lower Chao Phraya River Basin. The temporal distribution pattern of men monthly reference evapotranspiration is similar to the distribution pattern of temperature and net radiation. The mean monthly reference evapotranspiration is increasing from January to April but it is decreasing from April to December. Also temperature and net radiation are increasing from January to April but they are decreasing from April to December. The highest values of mean monthly reference evapotranspiration are found in April and the highest values of temperature and net radiation are respectively also found in May and April.

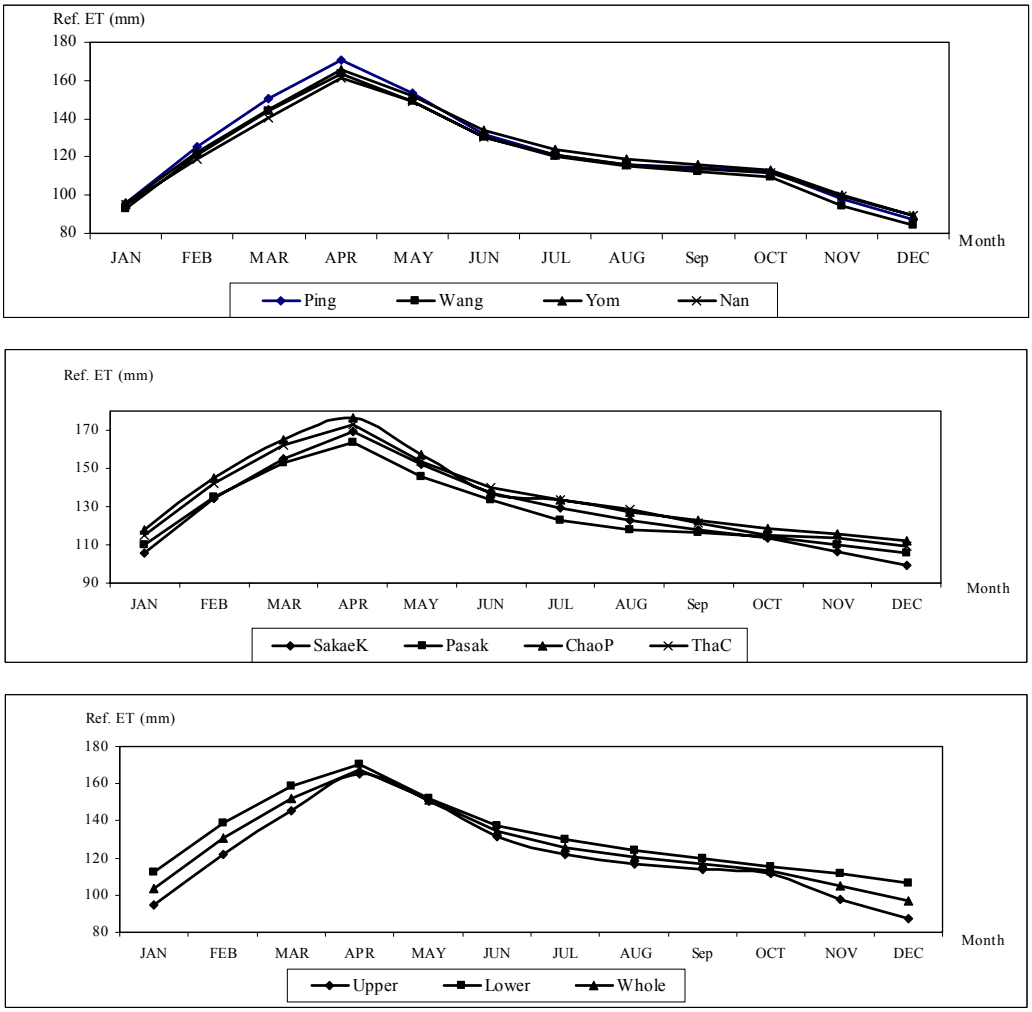

Figure 20 Mean monthly reference evapotranspiration in the Ping, Wang, Yom, Nan, Sakae Krang, Pasak, Chao Phraya, Tha Chin sub-basin and the upper, lower, and whole catchment of the Chao Phraya River Basin

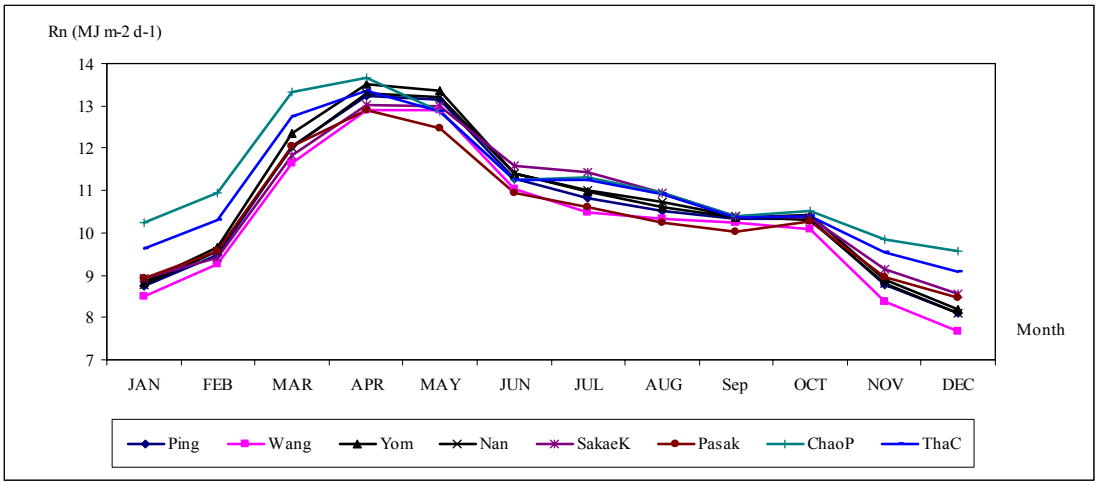

Figure 21 Mean monthly net radiation (Rn) in the Ping, Wang, Yom, Nan, Sakae Krang, Pasak, Chao Phraya, and Tha Chin sub-basin

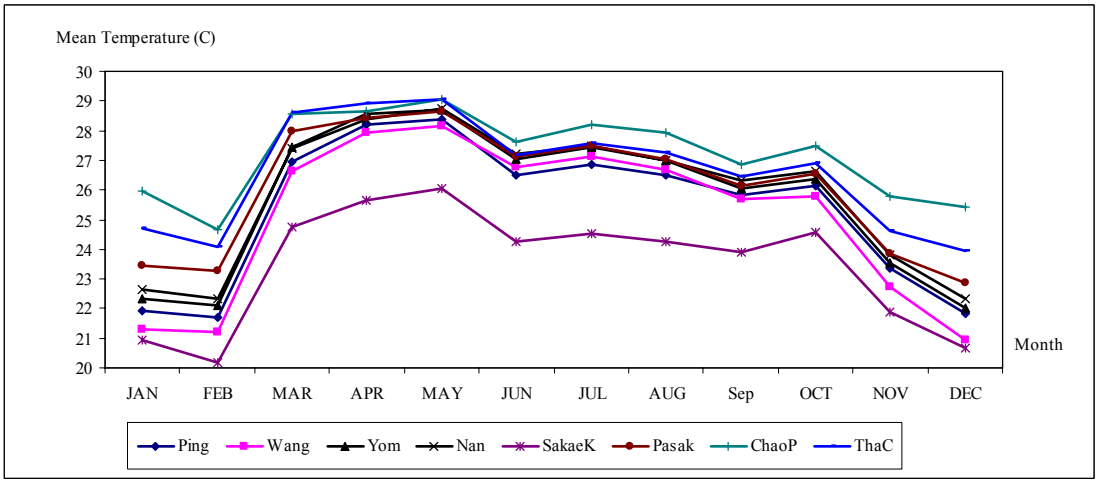

Figure 22 Mean monthly temperature in the Ping, Wang, Yom, Nan, Sakae Krang, Pasak, Chao Phraya, and Tha Chin sub-basin

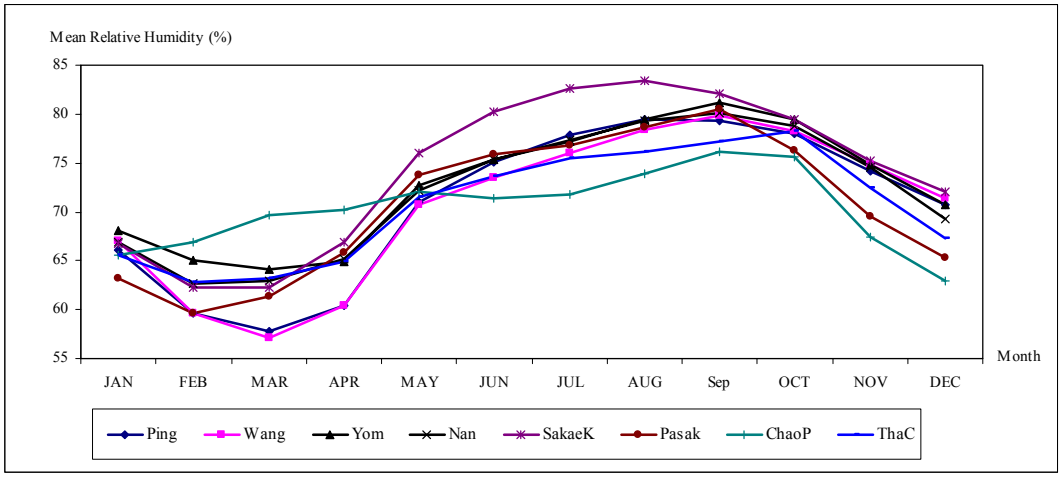

Figure 23 Mean monthly relative humidity in the Ping, Wang, Yom, Nan, Sakae Krang, Pasak, Chao Phraya, and Tha Chin sub-basin

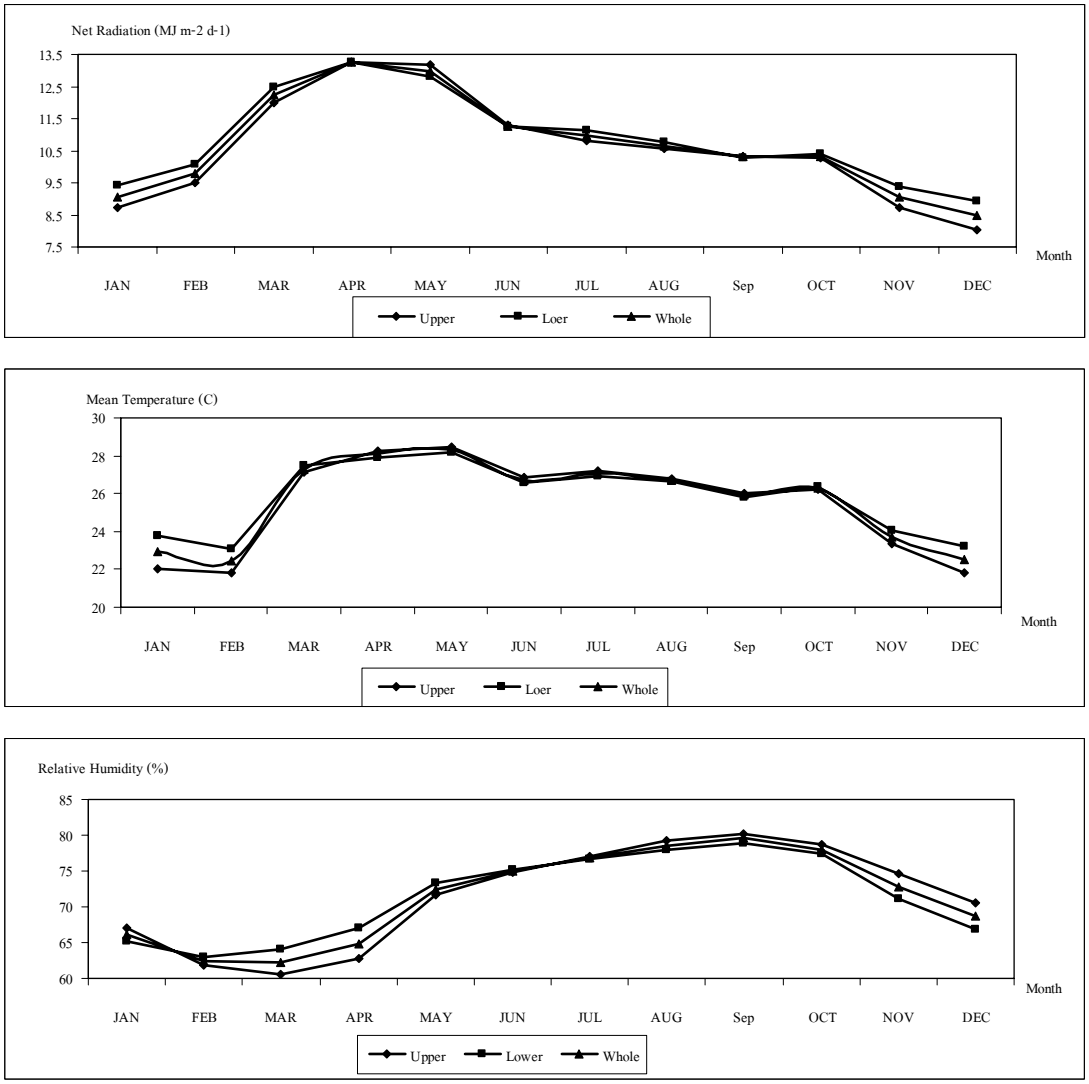

Figure 24 Mean monthly net radiation, temperature, and relative humidity in the upper, lower, and whole catchment of the Chao Phraya River Basin

Temporal Trends in Mean Annual Rainfall Obtained by Recorded rainfall

The time series of annual rainfall from 1971 and 2002 averaged over 8 sub-basins are plotted in Figure 25. It is seen that mean annual rainfall in the Ping, Wang, Yom, Nan, Sakae Krang and Pasak sub-basin have increased during a 32-year period while mean annual rainfall in the Chao Phraya and Tha Chin sub-basin have decreased during a 32-year period. The strongest and weakest of increasing trends are respectively in Nan and Ping sub-basin while the strongest and weakest of decreasing trends are in Chao Phraya and Tha Chin sub-basin, respectively.

Actual Evapotranspiration

SEBAL Script for MODIS and Landsat 7 Image

To calculate actual evapotranspiration using the concept of SEBAL, the script of this method was created using Spatial Modeler Language in ERDAS IMAGINE 8.5. There are two scripts from this study that are the script for MODIS image and the script for Landsat 7 image. Both scripts of MODIS image and Landsat 7 image are included the process of calculation presented in Figure 26. These scripts can be used for calculation the latent energy of evaporation (LE), the net radiation flux at the soil surface (R_n), the soil heat flux (G), the sensible heat flux to the air (H), the Evaporative Fraction (Λ), instantaneous actual evapotranspiration, and 24-hour actual evapotranspiration.

Addition, the relationship between actual evapotranspiration from MODIS image and Landsat 7 image was determined that is $Y = 0.707X+2.224$ ($R^2 = 0.668$) where Y is the actual evapotranspiration from Landsat 7 image and X is the actual evapotranspiration from MODIS image. This relationship was used to calibrate actual evapotranspiration from MODIS image for this study. Also, this relationship can be used for the calibration in other studies. The results are included 24-hour actual evapotranspiration from MODIS image and Landsat 7 image shown in Appendix Figure E1 –E2.

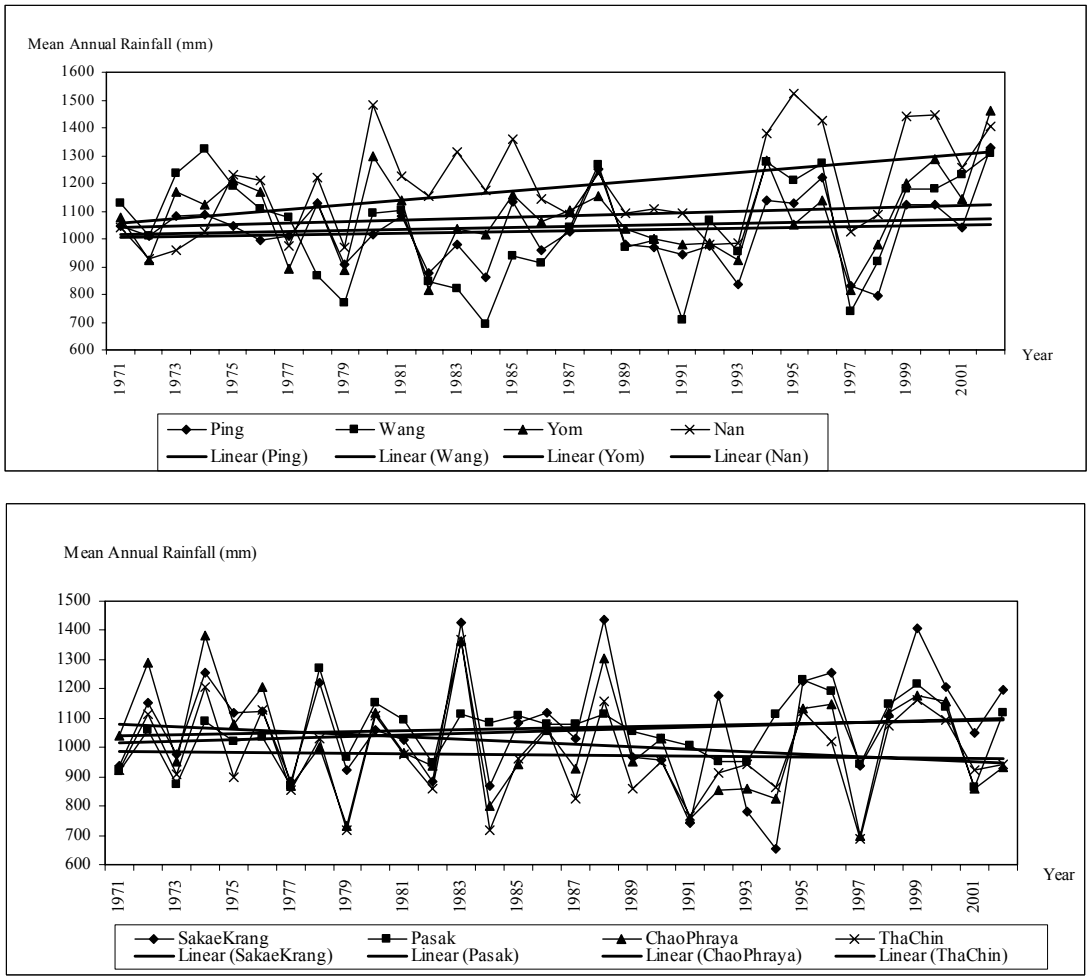

Figure 25 Mean annual rainfall and their linear trends in the Ping, Wang, Yom, Nan, Sakae Krang, Pasak, Chao Phraya, and Tha Chin sub-basin

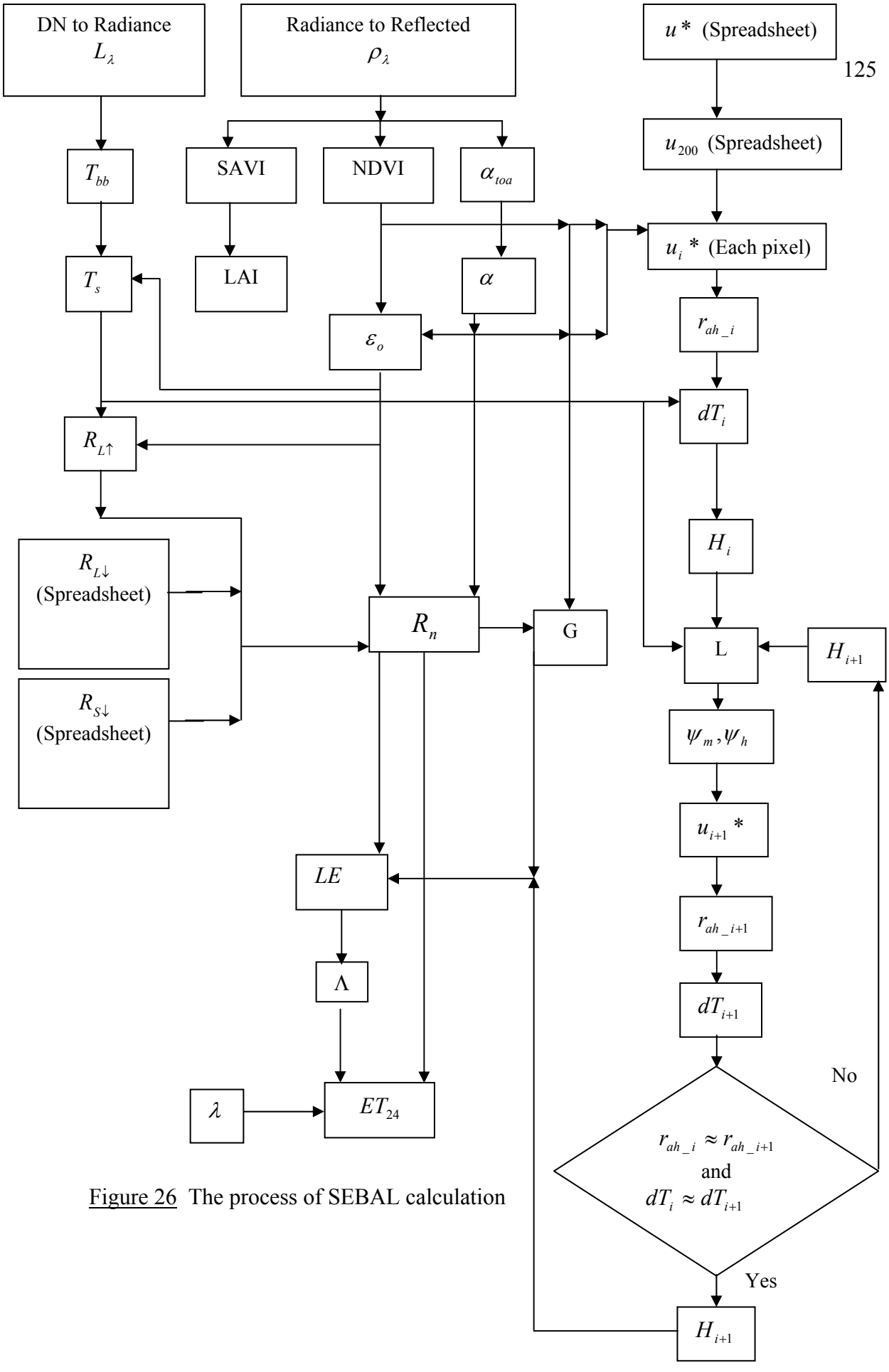

Figure 26 The process of SEBAL calculation

Spatial Distribution of Monthly Actual Evapotranspiration (Temporal) obtained by MODIS Image and Weather Data

The spatial distributions of monthly actual evapotranspiration (temporal) calculated using MODIS images and weather data are presented in Figure 27. This figure shows the changing of actual evapotranspiration from January to December. It is seen that, in January the highest value can be found in Ping and Sakae Krang sub-basin. In February, the highest value can be also found in Ping and Sakae Krang sub-basin and actual evapotranspiration, which is more than 60 mm, can be found in many areas. In March, the highest value can be also found in many areas of all eight sub-basins. Addition, actual evapotranspiration is mostly more than 70 mm. In April and May, the highest value can be found in many areas of Ping, Yom, Sakae Krang, Tha Chin, Chao Phraya, and Pasak sub-basin. Moreover, actual evapotranspiration is mostly more than 60 mm. During June to August, actual evapotranspiration that is more than 70 mm distributes in many areas of Ping, Yom, Sakae Krang, Tha Chin, Chao Phraya, and Pasak sub-basin. For other area, it is less than 50 mm. In September and October, actual evapotranspiration, which is more than 60 mm, can be found in many areas of all eight sub-basins. In November, the highest values can be found in Ping sub-basin. For other areas, actual evapotranspiration is mostly more than 70 mm. In December, actual evapotranspiration that is more than 70 mm distributes in many areas of Ping, Yom, Sakae Krang, Tha Chin, Chao Phraya, and Pasak sub-basin.

The temporal distributions of Ping, Wang, Yom, and Nan have increased during January to March, have decreased during March to July, have increased during July to November, and have decreased during November to December. For Sakae Krang, Pasak, Chao Phraya, and Tha Chin, the trend of temporal distributions have gradually increased during January to March and have gradually decreased during March to December.

The mean monthly actual evapotranspirations in Ping, Wang, Yom, Nan, Sakae Krang, Pasak, Chao Phraya, and Tha Chin sub-basin are 75.159, 62.700,

76.845, 65.090, 89.407, 78.916, 95.125, and 85.106 mm, respectively. On the one hand, the range of monthly actual evapotranspirations in Ping, Wang, Yom, Nan, Sakae Krang, Pasak, Chao Phraya, and Tha Chin sub-basin are 31.605-120.910, 33.188-95.519, 56.291-105.857, 44.824-89.640, 70.984-118.874, 63.963-104.702, 76.315-123.913, and 57.525-116.667 mm, respectively.

Addition, Figure 27 can be separated by the values of mean actual evapotranspiration and mean evaporation for each land use presented in Table 16. Table 16 shows mean actual evapotranspiration and mean evaporation in eight sub-basins. Mean actual evapotranspiration was considered in non-irrigated area (NI), forest (F), irrigated area (IA), and other plant (M). The non-irrigated areas are covered rice, maize, sugarcane, cassava, small vegetation, and fruit. The irrigated area, where are supported water by the irrigation project of Royal Irrigation Department, are also planted rice, maize, sugarcane, cassava, small vegetation, and fruit. These crops are mainly cultivated in both non-irrigated area and irrigated area. On the one hand, mean evaporation was concerned in urban (U) and reservoir (W).

Crop Coefficient for Rice, Maize, and Sugarcane

SEBAL and the FAO Penman-Monteith equation were used to determine crop coefficient for rice, maize, and sugarcane. Table 17 demonstrates the comparison of SEBAL and the FAO Penman-Monteith equation derived crop coefficient with the FAO crop coefficient (Allen *et al.*, 1998) and Table 18 presents the lengths of crop development stage for various planting periods. In Table 17, the average crop coefficients computed by SEBAL and the FAO Penman-Monteith equation for $K_{c,ini}$, $K_{c,mid}$ and $K_{c,late}$ are 0.963, 1.194 and 0.934 for rice, 0.978, 1.184 and 0.897 for maize and 0.811, 1.262 and 1.007 for sugarcane. On the other hand, the FAO crop coefficients for $K_{c,ini}$, $K_{c,mid}$ and $K_{c,late}$ are 1.050, 1.200, and 0.900 for rice, 0.500, 1.150, and 1.050 for maize and 0.410, 1.250, and 0.750 for sugarcane.

According to the results of this study, the estimated values of average crop coefficient by SEBAL and the FAO Penman-Monteith equation for rice are nearby the FAO crop coefficient with less than 0.10 differences. Also, the crop coefficients for Suphanburi 1, Chai Nat 1, Ko Kho 10, Ko Kho 7, and Pathumthanee 1 are nearby the FAO crop coefficient with less than 0.10 differences except the crop coefficients of Suphanburi 1 and Ko Kho 7 during initial stage that are underestimated the FAO crop coefficient by 0.167 and 0.193, respectively. On the other hand, the crop coefficients of this study for maize and sugarcane during the mid-season stage and the end of the late season stage are nearby the FAO crop coefficient with less than 0.30 differences. However, during the initial stage, the estimated crop coefficient values for maize and sugarcane are overestimated the FAO crop coefficient by 0.478 and 0.401, respectively. Above variations could be attributed to differences in crop varieties and crop age conditions, which are the different conditions for crop coefficient estimation between this study and the FAO. SEBAL and the FAO Penman-Monteith equation can be applied successfully to estimate and update crop coefficient curves for the large population of crop in the Chao Phraya River Basin.

Table 17 The crop coefficient for the rice, maize and sugarcane

Crop	Kc from this study			Kc from the FAO		
	Initial	Mid season	Late	Initial	Mid season	Late
Rice	0.963	1.194	0.934	1.050	1.200	0.900
- Suphanburi 1	0.883	1.146	0.999			
- Chai Nat 1	1.006	1.136	0.950			
- Ko Kho 10	1.073	1.245	0.963			
- Ko Kho 7	0.857	1.210	0.886			
- Pathumthanee 1	0.997	1.232	0.874			
Maize	0.978	1.184	0.897	0.500	1.150	1.050
Sugarcane	0.811	1.262	1.007	0.410	1.250	0.750

Table 18 The lengths of crop development stage for various planting periods

Unit: day

Crop	Initial	Development	Mid-Season	Late Season	Total
Rice	30	30	40	30	130
- Suphanburi 1	30	30	35	30	125
- Chai Nat 1	30	30	40	30	130
- Ko Kho 10	30	30	45	30	135
- Ko Kho 7	30	30	40	30	130
- Pathumthanee 1	30	30	35	30	125
Maize	20	30	40	30	120
Sugarcane	30	50	180	60	320

Rainfall

Spatial and Temporal Distribution of Monthly Rainfall Obtained by Recorded Rainfall and TRMM (3B42 V6) Images

The spatial distributions of monthly rainfall obtained by recorded rainfall and TRMM (3B42 V6) images are shown in Figure 28. It is seen that, in January, rainfall is mostly 0.00 – 20.00 mm. The highest rainfall found in Sakae Krang and Tha Chin sub-basin is about 30.00 – 50.00 mm. In February, rainfall is mostly 0.00 – 20.00 mm and there is rainfall more than 80.00 mm in small area of Sakae Krang sub-basin. In March, rainfall is mostly 0.00 – 40.00 mm, there is rainfall more than 100.00 mm in Ping, Yom, and Pasak sub-basin. In April, rainfall is mostly less than 70.00 mm. but rainfall in small area of Tha Chin sub-basin is more than 100.00 mm. In May, the highest rainfall (more than 220.00 mm.) is found in the upper region of Ping, Wang, Yom, and Nan sub-basin. The lower rainfall that is less than 220.00 mm is found in the lower Chao Phraya River Basin. In June, rainfall that is more than 100.00 mm. is found in some area of Ping, Yom, Nan, and Pasak. In July, rainfall is mostly 30.00 – 140.00 mm. and rainfall that is more than 140.00 mm. is found in Ping and Nan sub-basin. In August, rainfall is mostly more than 180.00 mm in all sub-basins. Addition, there is rainfall that is more than 400.00 mm. in Nan and Pasak sub-basin. In September, rainfall is less than 220.00 mm. in many areas but there is rainfall that is more than 220.00 mm. in small area of Sakae Krang. In October, rainfall is less than 140.00 mm. in many areas but there is rainfall that is more than 140.00 mm. in Ping, Yom, Sakae Krang, and Chao Phraya sub-basin. In November, the highest rainfall that is more than 100.00 mm. is found in Ping and Chao Phraya sub-basin. In December, rainfall is mostly 0.00 – 40.00 mm. in all sub-basin except in upper Ping sub-basin where there is rainfall more than 40.00 mm.

After the monthly rainfall for the study area was obtained using the monthly rainfall shown in Figure 28, the temporal distribution of monthly rainfall is plotted as Figure 29. It is seen that the temporal distribution pattern for all sub-basins is similar. The monthly rainfall is gradually increasing from January to May and is decreasing in June. From June to September, the monthly rainfall is gradually increasing. Thereafter, the monthly rainfall is rapidly decreasing from September to December. The highest monthly rainfall is in September for Ping, Wang, Yom, Sakae Krang, Pasak, Chao Phraya, and Tha Chin sub-basin while the highest monthly rainfall for Nan is in August. The lowest monthly rainfall is in January and December for eight sub-basins.

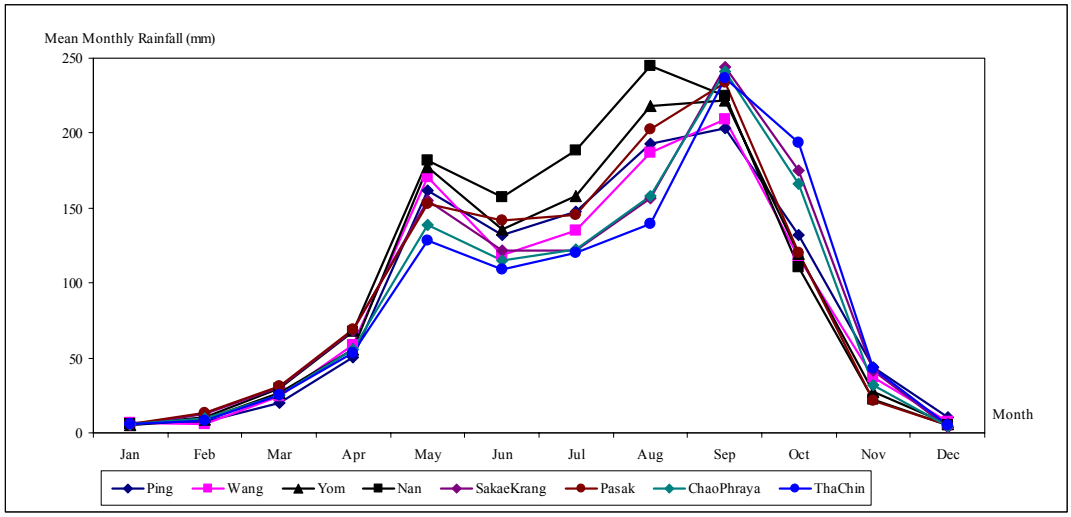

Figure 29 Mean monthly rainfall in the Ping, Wang, Yom, Nan, Sakae Krang, Pasak, Chao Phraya, and Tha Chin sub-basin

Addition, rainfall in Figure 28 can be separated for each land use presented in Table 19. Table 19 shows mean monthly rainfall in eight sub-basins.

Water Budget

Spatial Distribution of the Irrigation Requirement

Since monthly rainfall and monthly actual evapotranspiration for the Chao Phraya River Basin are results of this study, these results can be utilized to determine the irrigation requirement presented in Figure 30. Figure 30 shows spatial distribution of the irrigation requirement from January to December. To calculate the irrigation requirement rainfall is subtracted by actual evapotranspiration. This irrigation requirement can be positive value and negative value. The positive value means that there is excess water while the negative value means that there is insufficient water.

Figure 30 is seen that during January and February there is insufficient water in all eight sub-basins. In March, there is insufficient water in all eight sub-basins except in some areas of Ping, Nan, and Sakae Krang sub-basin. The highest insufficient water can be found in Ping, Yom, Tha Chin, and Chao Phraya sub-basin. For April, there are both an excess water and an insufficient water. An excess water can be found in some areas of Ping, Yom, Nan, Tha Chin, and Pasak sub-basin but other areas consist of an insufficient water. The highest insufficient water can be found in Yom, Nan, Tha Chin, and Chao Phraya sub-basin. For May, many areas are included an excess water and the highest excess water can be found in Ping, Wang, Yom, and Nan sub-basin. However, there is an insufficient water in some areas, where are Yom, Nan, Tha Chin, and Chao Phraya sub-basin. During June and July, many areas are consisted of excess water except in some areas of Yom, Nan, Sakae Krang, Pasak, Tha Chin, and Chao Phraya sub-basin. In August, there is excess water in all eight sub-basins and the highest excess water can be found in Yom, Nan, and Pasak sub-basin. In September, all eight sub-basins are obtained excess water and there is a small different value between excess water in each sub-basin. In October, many areas are excess water except in some areas of Ping, Nan, Tha Chin, Chao Phraya, and Pasak sub-basin. In November, there are both excess water and insufficient water. Excess water can be found in Ping Nan, and Pasak sub-basin. Addition, some areas of Wang, Yom, Sakae Krang, Tha Chin, and Chao Phraya sub-

basin consists of excess water. Insufficient water can be found in some area of Wang, Yom, Sakae Krang, Tha Chin, and Chao Phraya sub-basin. For December, all areas of eight sub-basins are included an insufficient water except in small area of Ping, Yom, and Nan sub-basin.

In addition, the irrigation requirement in Figure 30 can be indicated by land use presented in Table 20. This table shows the irrigation requirement in eight sub-basins. It is seen that, during January to April, rainfall over the Chao Phraya River Basin is less than actual evapotranspiration. In May, rainfall over the Chao Phraya River Basin is more than actual evapotranspiration except in irrigated area, water, and non-irrigated area of Sakae Krang, and Tha Chin, respectively. In June and July, rainfall is more than actual evapotranspiration in the upper Chao Phraya River Basin but rainfall is less than actual evapotranspiration in many areas of the lower Chao Phraya River basin. During August to October, rainfall over the Chao Phraya River Basin is more than actual evapotranspiration. In November and December, rainfall is less than actual evapotranspiration in many areas.

Furthermore, Table 20 is presented the summation of annual irrigation requirement in all eight sub-basins. It is seen that Ping, Wang, and Yom sub-basin consist of the positive values of the annual irrigation requirement in all land use. It means that there is excess water in these three sub-basins. For Nan, Sakae Krang, and Pasak sub-basin, they are included by the positive values of the annual irrigation requirement in all land use except in irrigated area. It means that irrigated area in these three sub-basins need more water to support insufficient water. For Tha Chin and Chao Phraya sub-basin, the summations of the annual irrigation requirement are negative values for all land use. It means that it is necessary to support water to these two sub-basins.

Monthly Water Budget Calculation

The results of monthly water budget calculation are presented in Table 21 – 27. Table 21 can be seen that there is water shortage in January, February, March, April, and December that are -2110.5, -3238.0, -3741.3, -1672.0, and -1704.0 million m^3 (MCM), respectively. During May to November, there is excess water that are 4096.0, 606.2, 1160.8, 4240.0, 1548.8, 563.8, and 250.3 MCM, respectively. An annual subsurface outflow is 9716.4 MCM. The highest values of subsurface outflow can be found in May that is 3162.5 MCM. The significance level of the result is 81.99 %.

Table 21 The water budget calculation in Ping sub-basin

Unit: MCM

Month	Inflow			Outflow			ΔS
	Rain	Qsi	Qssi	ETc	Qso	Qsso	
1	183.8	34.1	-70.2	2200.6	493.8	-436.1	-2110.5
2	319.2	21.3	27.7	2773.7	634.8	197.7	-3238.0
3	735.9	15.4	-36.8	3286.5	909.0	260.3	-3741.3
4	1276.3	6.2	-161.9	2084.0	718.1	-9.5	-1672.0
5	8498.4	37.1	1414.1	1987.2	704.0	3162.5	4096.0
6	3351.6	70.3	2.8	1359.9	385.5	1073.1	606.2
7	3378.0	31.6	58.9	888.9	405.0	1013.8	1160.8
8	7768.4	104.4	1249.2	1360.7	371.0	3150.2	4240.0
9	5973.3	874.8	12.3	1802.6	2406.3	1102.8	1548.8
10	3460.3	290.3	-55.7	2063.6	1266.0	-198.4	563.8
11	5089.9	316.4	35.5	2822.0	2081.9	287.6	250.3
12	1455.1	151.6	-60.7	2006.9	1130.7	112.4	-1704.0
Sum	41490.1	1953.6	2415.3	24636.5	11506.1	9716.4	0.0
	t	0.982					
	df	22					
Significance level		81.99%					

Table 22 can be seen that there is water shortage in January, February, March, April, November, and December that are -481.2, -702.8, -692.0, -145.9, -160.3, and -409.7 MCM, respectively. During May to October, there is excess water that are 828.2, 255.2, 479.6, 727.0, 157.4, and 144.5 MCM, respectively. An annual subsurface outflow is 3265.1 MCM. The highest values of subsurface outflow can be found in May that is 1487.4 MCM. The significance level of the result is 88.76 %.

Table 22 The water budget calculation in Wang sub-basin

Unit: MCM

Month	Inflow			Outflow			ΔS
	Rain	Qsi	Qssi	ETc	Qso	Qsso	
1	84.3	0.0	0.0	533.8	34.1	-2.5	-481.2
2	36.4	0.0	0.0	614.4	21.3	103.5	-702.8
3	239.0	0.0	0.0	849.6	15.4	66.1	-692.0
4	377.3	0.0	0.0	603.6	6.2	-86.7	-145.9
5	2936.0	0.0	0.0	583.3	37.1	1487.4	828.2
6	743.8	0.0	0.0	366.6	70.3	51.7	255.2
7	913.3	0.0	0.0	301.2	31.6	100.8	479.6
8	2597.7	0.0	0.0	457.8	104.4	1308.5	727.0
9	1714.7	0.0	0.0	595.8	874.8	86.6	157.4
10	937.7	0.0	0.0	495.2	290.3	7.8	144.5
11	1148.9	0.0	0.0	854.2	316.4	138.6	-160.3
12	238.1	0.0	0.0	492.9	151.6	3.3	-409.7
Sum	11967.0	0.0	0.0	6748.3	1953.6	3265.1	0.0
t		1.269					
df		22					
Significance level		88.76%					

Table 23 can be seen that there is water shortage in January, February, March, April, September, October, November, and December that are -842.1, -1381.3, -1309.0, -1201.3, -30.9, -79.6, -372.8, and -591.7 MCM, respectively. During May to August, there is excess water that are 2503.6, 152.4, 707.3, and 2445.4 MCM, respectively. An annual subsurface outflow is 6531.8 MCM. The highest values of subsurface outflow can be found in August that is 2684.7 MCM. The significance level of this result is 86.89 %.

Table 23 The water budget calculation in Yom sub-basin

Unit: MCM

Month	Inflow			Outflow			ΔS
	Rain	Qsi	Qssi	ETc	Qso	Qsso	
1	314.7	0.0	0.0	1034.6	34.2	88.0	-842.1
2	42.7	0.0	0.0	1321.9	13.1	89.0	-1381.3
3	880.5	0.0	0.0	1990.1	27.8	171.5	-1309.0
4	631.2	0.0	0.0	1516.9	11.2	304.5	-1201.3
5	6271.9	0.0	0.0	1778.7	73.8	1915.8	2503.6
6	2074.3	0.0	0.0	1174.4	243.2	504.2	152.4
7	2723.4	0.0	0.0	904.2	215.8	896.1	707.3
8	6983.6	0.0	0.0	1381.2	472.2	2684.7	2445.4
9	4062.6	0.0	0.0	1466.0	2446.1	181.4	-30.9
10	3142.8	0.0	0.0	1152.8	2026.3	43.3	-79.6
11	1919.6	0.0	0.0	1551.7	913.6	-172.9	-372.8
12	637.0	0.0	0.0	872.6	530.0	-173.8	-591.7
Sum	29684.2	0.0	0.0	16145.0	7007.4	6531.8	0.0
	t	1.189					
	df	22					
Significance level		86.89%					

Table 24 can be seen that there is water shortage in January, February, March, April, September, October, November, and December that are -1102.1, -1961.5, -2093.5, -1223.17, -1073.3, -1065.2, -1857.9, and -456.9 MCM, respectively. During May to August, there is excess water that are 3220.5, 478.4, 2168.4, and 4965.2 MCM, respectively. An annual subsurface outflow is 6089.7 MCM. The highest values of subsurface outflow can be found in August that is 2089.4 MCM. The significance level of this result is 76.36 %.

Table 24 The water budget calculation in Nan sub-basin

Unit: MCM

Month	Inflow			Outflow			ΔS
	Rain	Qsi	Qssi	ETc	Qso	Qsso	
1	498.6	0.0	0.0	849.0	646.9	104.8	-1102.1
2	22.7	0.0	0.0	1178.3	692.3	113.6	-1961.5
3	716.4	0.0	0.0	1727.4	893.6	188.8	-2093.5
4	1379.8	0.0	0.0	1461.2	976.7	164.9	-1223.2
5	7193.9	0.0	0.0	1624.9	928.9	1419.6	3220.5
6	2970.1	0.0	0.0	1010.8	902.6	578.3	478.4
7	4843.1	0.0	0.0	772.0	963.7	939.0	2168.4
8	9915.8	0.0	0.0	1063.5	1797.6	2089.4	4965.2
9	3930.0	0.0	0.0	1141.6	3722.6	139.1	-1073.3
10	2864.6	0.0	0.0	922.5	2889.3	117.9	-1065.2
11	1405.3	0.0	0.0	1329.5	1793.6	139.1	-1856.9
12	913.0	0.0	0.0	656.3	618.6	95.0	-456.9
Sum	36653.1			13737.0	16826.4	6089.7	0.0
	t	0.744					
	df	22					
Significance level		76.36%					

Table 25 can be seen that there is water shortage in January, February, March, April, November, and December that are -185.5, -200.3, -275.3, -95.3, -61.6, and -207.0 MCM, respectively. During May to October, there is excess water that are 124.5, 49.7, 10.1, 382.8, 230.9, and 227.1 MCM, respectively. An annual subsurface outflow is 1312.7 MCM. The highest values of subsurface outflow can be found in September that is 362.6 MCM. The significance level of this result is 93.71 %.

Table 25 The water budget calculation in Sakae Krang sub-basin

Unit: MCM

Month	Inflow			Outflow			ΔS
	Rain	Qsi	Qssi	ETc	Qso	Qsso	
1	121.6	0.0	0.0	273.5	0.0	33.6	-185.5
2	159.5	0.0	0.0	326.2	0.0	33.6	-200.3
3	183.2	0.0	0.0	426.8	0.0	31.7	-275.3
4	294.9	0.0	0.0	343.4	0.0	46.8	-95.3
5	672.0	0.0	0.0	405.6	0.0	141.9	124.5
6	442.6	0.0	0.0	307.2	13.1	72.6	49.7
7	303.2	0.0	0.0	226.4	22.7	44.0	10.1
8	925.0	0.0	0.0	272.5	27.2	242.5	382.8
9	1055.1	0.0	0.0	266.8	194.8	362.6	230.9
10	971.8	0.0	0.0	250.2	278.6	215.9	227.1
11	397.8	0.0	0.0	295.9	129.7	33.8	-61.6
12	99.1	0.0	0.0	223.0	29.3	53.8	-207.0
Sum	5625.6	0.0	0.0	3617.6	695.3	1312.7	0.0
t		1.615					
df		22					
Significance level		93.71%					

Table 26 can be seen that there is water shortage in January, February, March, April, September, October, November, and December that are -683.2, -836.2, -239.6, 394.1, -144.0, -483.6, -629.1, and -421.7 MCM, respectively. During May to August, there is excess water that are 636.9, 217.2, 241.3, and 2736.1 MCM, respectively. An annual subsurface outflow is 3092.9 MCM. The highest values of subsurface outflow can be found in May that is 802.1 MCM. The significance level of this result is 79.99 %.

Table 26 The water budget calculation in Pasak sub-basin

Unit: MCM

Month	Inflow			Outflow			ΔS
	Rain	Qsi	Qssi	ETc	Qso	Qsso	
1	109.8	0.0	0.0	632.5	99.0	61.5	-683.2
2	107.4	0.0	0.0	759.7	123.3	60.5	-836.2
3	1065.9	0.0	0.0	994.3	88.3	222.9	-239.6
4	879.0	0.0	0.0	944.3	167.8	160.9	-394.1
5	2661.1	0.0	0.0	1109.9	112.1	802.1	636.9
6	1290.0	0.0	0.0	759.0	25.1	288.8	217.2
7	1359.7	0.0	0.0	671.9	149.8	296.7	241.3
8	4244.1	0.0	0.0	736.2	52.1	719.7	2736.1
9	2798.8	0.0	0.0	640.2	2076.1	226.4	-144.0
10	1266.3	0.0	0.0	643.9	983.4	122.5	-483.6
11	594.0	0.0	0.0	904.9	244.4	73.8	-629.1
12	341.8	0.0	0.0	589.5	116.9	57.1	-421.7
Sum	16717.5	0.0	0.0	9386.3	4238.4	3092.9	0.0
	t	0.897					
	df	22					
Significance level		79.99%					

Table 27 can be seen that there is water shortage in January, February, March, April, and December that are -3179.1, -3400.3, -3796.2, -2726.5, and -568.4 MCM, respectively. During May to November, there is excess water that are 4396.0, 484.8, 755.7, 5036.4, 1238.1, 636.5, and 1123.0 MCM, respectively. An annual subsurface outflow is 32651.4 MCM. The significance level of this result is 98.05 %.

Table 27 The water budget calculation in Chao Phraya and Tha Chin sub-basin

Unit: MCM

Month	Inflow			Outflow			ΔS
	Rain	Qsi	Qssi	ETc	Qso	Qsso	
1	126.4	993.8	-826.5	2639.1	227.7	606.1	-3179.1
2	52.1	1131.1	-323.9	3259.9	205.6	794.1	-3400.3
3	469.7	1490.0		4363.5	227.7	980.1	-3796.2
4	649.3	1482.4	-157.7	3820.3	220.3	659.9	-2726.5
5	2981.5	1423.6	6550.9	4212.3	227.7	2120.1	4396.0
6	1658.5	1302.9	1883.9	3277.4	220.3	862.9	484.8
7	1405.7	1443.3	2681.0	3060.2	227.7	1486.5	755.7
8	4353.7	2031.8	8227.9	3612.9	227.7	5736.5	5036.4
9	4145.6	8363.2	1301.8	2831.5	220.3	9520.7	1238.1
10	2179.8	9198.0	-380.9	2724.4	227.7	7408.4	636.5
11	1567.1	5517.1	-524.5	3264.3	220.3	1952.1	1123.0
12	560.6	2536.6	-462.3	2451.4	227.7	524.1	-568.4
Sum	20150.1	36914.0	17785.0	39517.1	2680.6	32651.4	0.0
	t	2.233					
	df	22					
Significance level		98.05%					

CONCLUSION AND RECOMMENDATION

As above the calculation and result of this study, it can be concluded as following.

1. In the Chao Phraya River Basin, the FAO Penman-Monteith method is suitable to calculate monthly reference evapotranspiration because this equation is affected by principal weather parameters and these weather parameters were collected by Thailand Meteorological Department (TMD) from 1971 to present. Also there is a strong correlation coefficient between the mean monthly reference evapotranspiration calculated from the FAO Penman-Monteith method and the mean monthly pan evaporation measured from TMD. As above, it is the strength of the FAO Penman-Monteith method in the Chao Phraya River Basin. However, since weather stations in the Chao Phraya River Basin are normally located in plain area, reference evapotranspiration from the FAO Penman-Monteith method in the Chao Phraya River Basin is reference evapotranspiration for plain area. To determine reference evapotranspiration in mountainous area, co-Kriging interpolation should be used. Addition, the estimation of reference evapotranspiration in mountainous area can be obtained by the technology of satellite image such as MODIS and Landsat 7.

2. After daily reference evapotranspiration was calculated by using the FAO Panman-Monteith method, the temporal trends in the time series of the mean annual reference evapotranspiration and mean annual pan evaporation during 1971-2002 in eight sub-basins of the Chao Phraya River Basin were analyzed. It presents that the trends of both mean annual reference evapotranspiration and mean annual pan evaporation in all the regions have decreased from 1971 to 2002. These decreasing trends relate to the decreasing trend of net radiation and the increasing trends of both temperature and relative humidity. The decreasing trend in mean annual reference evapotranspiration and mean annual pan evaporation differs in different regions.

3. Spatial distributions of mean monthly reference evapotranspiration were computed. It can be concluded that the highest value are found in the lower Chao

Phraya River Basin during January to December. The lower values of spatial distribution of mean monthly reference evapotranspiration from January to December are found in the upper Chao Phraya River Basin. The spatial distribution pattern in this study presents valuables information for regional hydrological studies because it is one of the most important factors to determine actual evapotranspiration.

Temporal distributions of mean monthly reference evapotranspiration present that the lowest value are found in the upper Chao Phraya River Basin during January to December. The highest values of temporal distribution of mean monthly reference evapotranspiration from January to December are found in the lower Chao Phraya River Basin. Temporal distributions of mean monthly reference evapotranspiration are effected by the meteorological variables especially temperature and net radiation because the temporal distribution pattern of mean monthly reference evapotranspiration is similar to the temporal distribution pattern of temperature and net radiation.

The changing of meteorological variable in each month and in different region will have a different effect on monthly reference evapotranspiration. As above result, the combination between the spatial and temporal distributions of monthly reference evapotranspiration and the spatial and temporal distributions of meteorological variables should be studied because it will provide an important background and physical interpolation to study climate change in the region.

Spatial and temporal reference evapotranspiration from this study can be applied to manage water. To use this spatial reference evapotranspiration or reference evapotranspiration map for each month (temporal), users have to know coordinate and crop type of their area because coordinate and crop type are used for determination monthly reference evapotranspiration and crop coefficient. Thereafter, actual evapotranspiraton, which is actual water demand, will be calculated and applied for design released water to agricultural area or irrigated area.

4. The spatial distributions of monthly actual evapotranspiration from this study can be concluded that actual evapotranspiration in the lower Chao Phraya River Basin is more than that in the upper Chao Phraya River basin during January to December. Then, the lowest value of spatial distribution of monthly actual evapotranspiration is found upper Chao Phraya River Basin during January to December. On the one hand, the highest value of spatial distribution of monthly actual evapotranspiration is found in Ping sub-basin during January to March, in lower Chao Phraya River Basin during April to August, in Yom sub-basin during September, and in Ping sub-basin and lower Chao Phraya River Basin during October to December. The mean monthly actual evapotranspirations in Ping, Wang, Yom, Nan, Sakae Krang, Pasak, Chao Phraya, and Tha Chin sub-basin are 75.159, 62.700, 76.845, 65.090, 89.407, 78.916, 95.125, and 85.106 mm, respectively.

Addition, total actual evapotranspiration is mostly found in forest, non-irrigated area, and irrigated area for eight sub-basins. For Ping and Wang sub-basin, the highest value can be found in the area of forest while the highest value of Yom, Nan, Sakae Krang, and Pasak sub-basin can be found in the area of non-irrigation. For Chao Phraya and Tha Chin sub-basin, the highest value can be found irrigated area. The lower value of Ping and Wang sub-basin can be found in the area of non-irrigation while the lower value of Yom, Nan, Sakae Krang, and Pasak sub-basin can be found in the area of forest. For Chao Phraya and Tha Chin sub-basin, the lower value can be found in non-irrigated area. On the other hand, the lowest total annual actual evapotranspiration in Ping, Yom, and Sakae Krang sub-basin is the value of other plant while the lowest total annual actual evapotranspiration in Wang, Nan, Pasak, Chao Phraya, and Tha Chin sub-basin is total evaporation in reservoir.

Then, it is necessary to concern actual evapotranspiration in forest, non irrigated, and irrigated area when water budget of basin and sub-basin is computed. However, it is difficult to determine actual evapotranspiration in forest because forest is mostly in mountain area. Also, there is insufficient weather station in mountain area so satellite image, such as MODIS and Landsat 7 image, is interesting to apply for actual evapotranspiration calculation.

5. The average crop coefficient calculation can be presented by the value of $K_{c,ini}$, $K_{c,mid}$ and $K_{c,late}$ for each crop and the result are 0.963, 1.194 and 0.934 for rice, 0.978, 1.184 and 0.897 for maize and 0.811, 1.262 and 1.007 for sugarcane. The computation of the crop coefficient displays that there is a potentiality in both SEBAL and the FAO Penman-Monteith equation to define the crop coefficient and even developing a new crop coefficient curve for new crop varieties for specific locations. The study also presents that the real-time and accurate remotely sensed measurements prepare irrigation managers and farmer with information that available, that information can enhance irrigation performance for sustainable management of limited water resources.

6. The time series of annual rainfall from 1971 and 2002 averaged over eight sub-basins are seen that temporal trends of mean annual rainfall in the Ping, Wang, Yom, Nan, Sakae Krang and Pasak sub-basin have increased during a 32-year period while temporal trends of mean annual rainfall in the Chao Phraya and Tha Chin sub-basin have decreased during a 32-year period. For spatial distribution of mean monthly rainfall in 2002, it can be concluded that the highest mean monthly rainfall or heavy rainfall can be found in some area of the Chao Phraya River Basin while the mean monthly rainfall of other areas are gradually change. Furthermore, the temporal distribution pattern for all sub-basins is similar. The mean monthly rainfall is gradually increasing from January to May and is decreasing in June. From June to September, the mean monthly rainfall is gradually increasing. Thereafter, the mean monthly rainfall is rapidly decreasing from September to December. The highest mean monthly rainfall is in September for Ping, Wang, Yom, Sakae Krang, Pasak, Chao Phraya, and Tha Chin sub-basin while the highest mean monthly rainfall for Nan is in August. The lowest mean monthly rainfall is in January and December for eight sub-basins.

7. As monthly rainfall and monthly actual evapotranspiration were utilized to concerned water budget calculation, the result of this calculation can be concluded that there is water shortage during dry season (January, February, March, April,

November, and December) while there is excess water during wet season (May to October). In addition, in Ping, Wang, Yom, Nan, Sakae Krang, and Pasak sub-basin, the summation of annual rainfall is more than the summation of annual actual evapotranspiration for all land use while, in Chao Phraya and Tha Chin sub-basin, the summation of annual rainfall is less than the summation of annual actual evapotranspiration for all land use. It means that, in Ping, Wang, Yom, Nan, Sakae Krang, and Pasak sub-basin, rainfall can support actual evapotranspiration if the excess water during wet season is storage to release during dry season. However, it is important to consider water loss from runoff and infiltration. For Chao Phraya and Tha Chin sub-basin, rainfall cannot support actual evapotranspiration so these sub-basins should be supported water from other sub-basin.